Chemical forces and self-assembly

Structures and Applications of self-assembled monolayers and multilayers

Outline

- Basic Structures
  - Langmuir Monolayers
  - Self-Assembled Monolayers (SAMS)
    - → Carboxylic acids on oxide surfaces
    - → Alkylsilanes on hydroxylated surfaces
    - → Organothiol on coinage metals
  - Mixed monolayers
  - Multilayers
  - Monolayer-protected clusters(MPCs)
- Applications of SAMs
  - Soft lithography
  - Dip-pen nanolithography
  - Sensor applications
  - Molecular electronics
  - etc

Langmuir monolayer

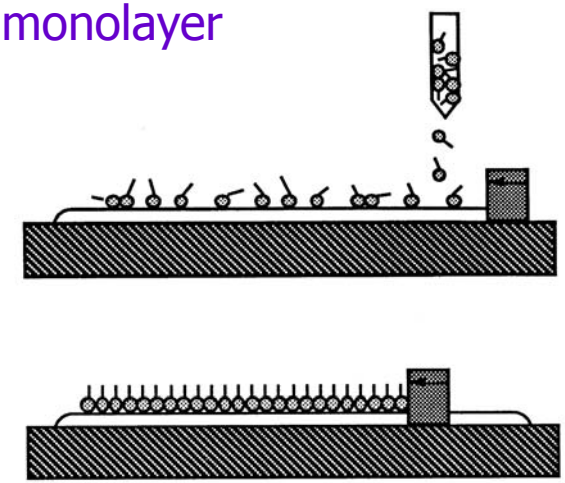

A monolayer of molecules in a two-dimensional gas (top), and in the compressed form (bottom).

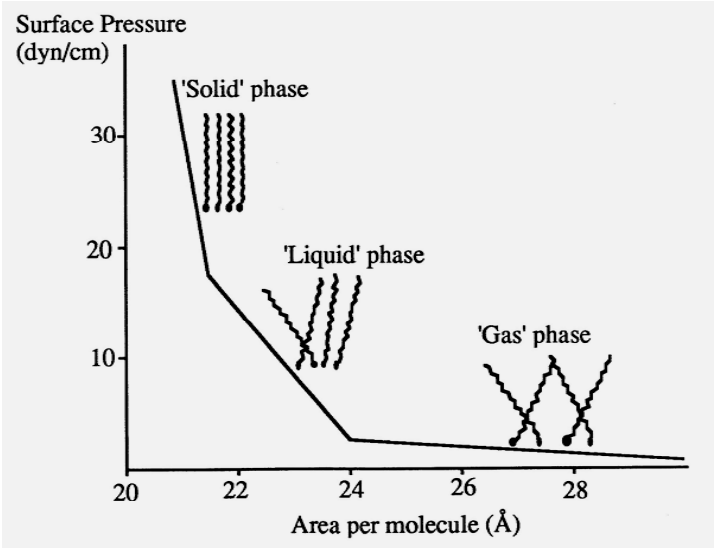

A scheme of surface pressure (π) vs. area per molecule (Å) for stearic acid on 0.01M HCl.

Langmuir-Blodgett Films

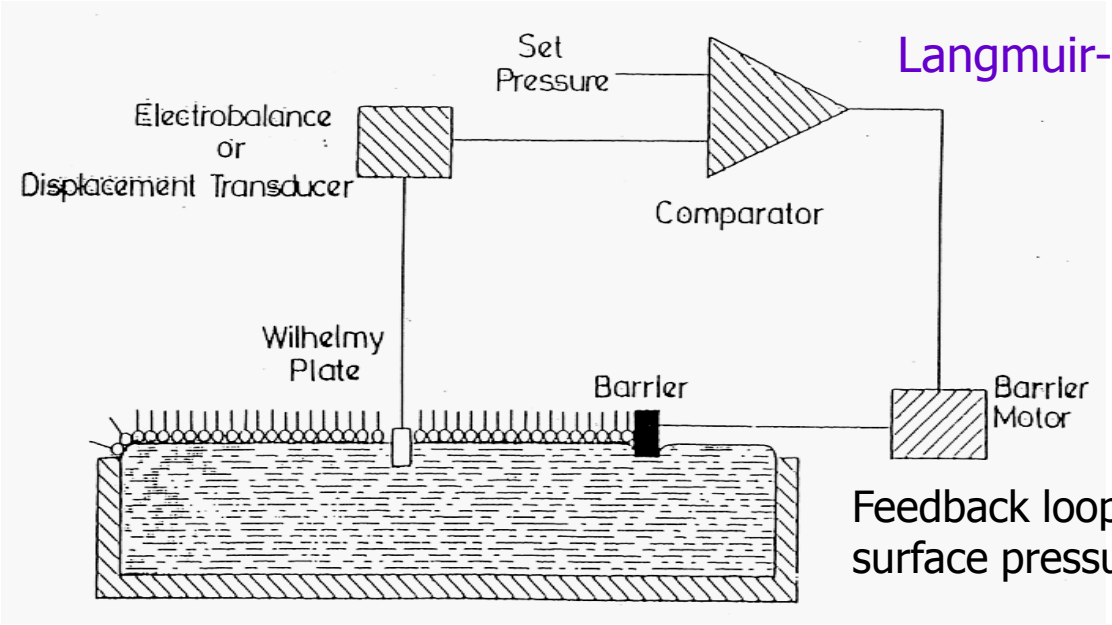

Feedback loop to control monolayer surface pressure.

Amphiphiles: A molecule that is insoluble in water, with one end that is hydrophilic and therefore preferentially resides in water, and the other end is hydrophobic and preferentially resides in air.

Very weak (no film)	Weak (unstable)	Strong (stable w C16)	Very strong (C16 cpd dissolve)
Hydrocarbon	$-CH_2OCH_3$	$-CH_2OH$; $-C_6H_4OH$	$-SO_3^-$
$-CH_2I$	$-C_6H_4OCH_3$	$-CN$; $-CH_2COCH_3$	$-SO_4^-$
$-CH_2Br$	$-COOCH_3$	$-COOH$; $-NHCONH_2$	$-C_6H_4SO^{4-}$
$-CH_2Cl$		$-CONH_2$	$-NR_4^+$
$-NO_2$		$-CH=NOH$	

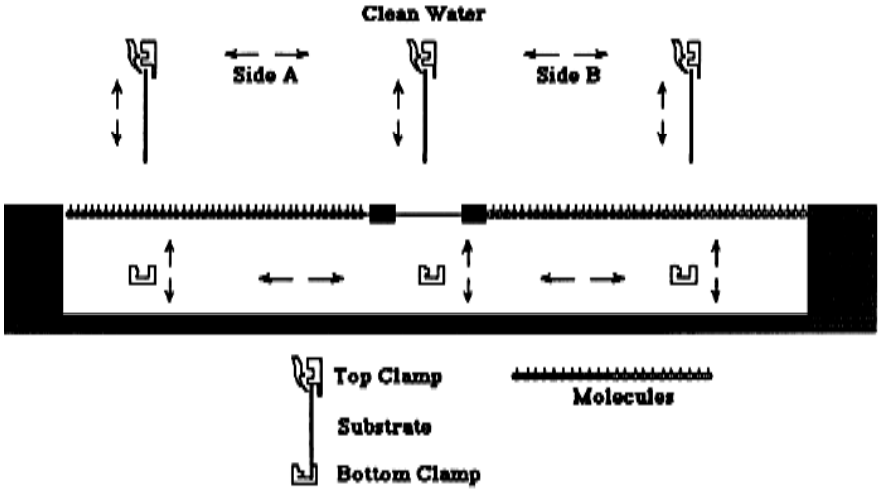

A cross-section view of LB film deposition in the KSV 5000 trough.

The deposition cycle in the KSV 5000 trough.

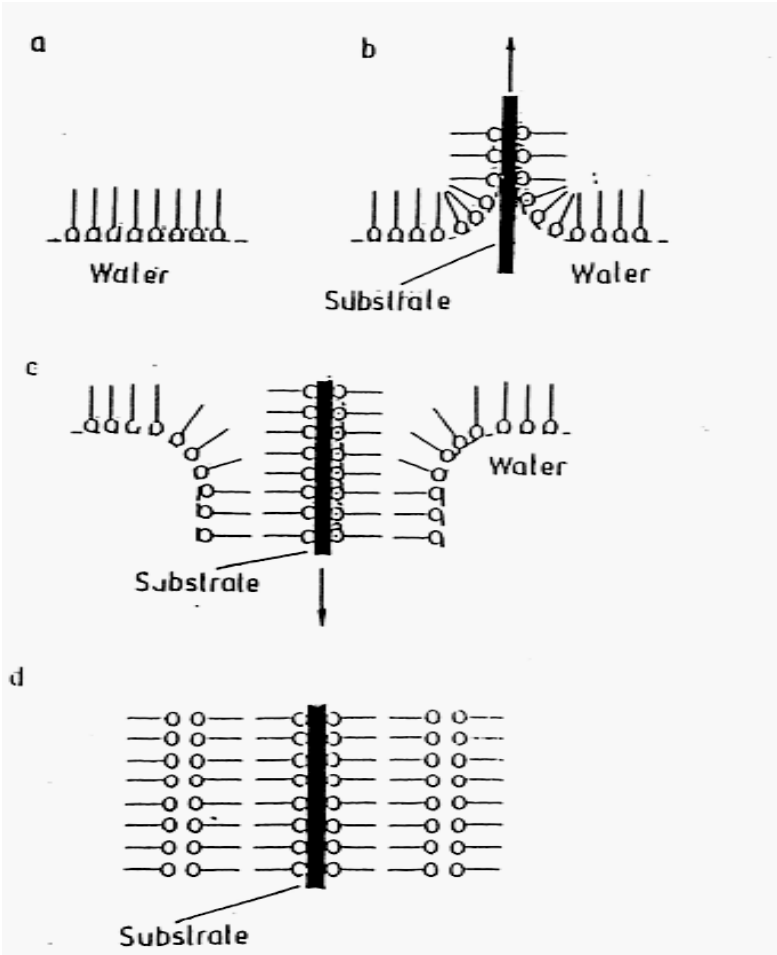

Y-type Langmuir-Blodgett film deposition.

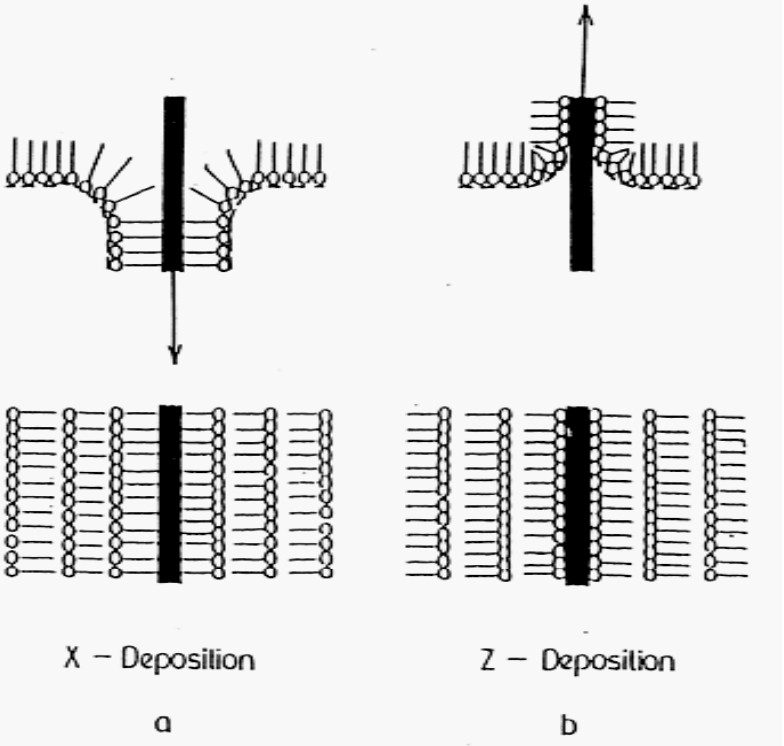

(a) X-type deposition. (b) Z-type deposition.

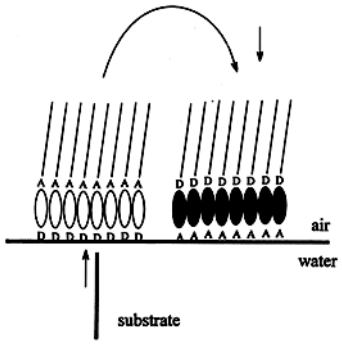

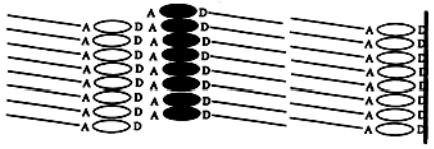

Figure 6.

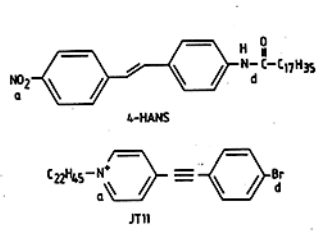

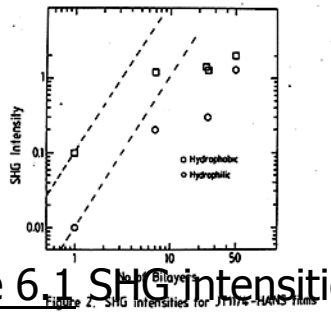

Figure 6.1 SHG intensities for JT11/4-HANS films.

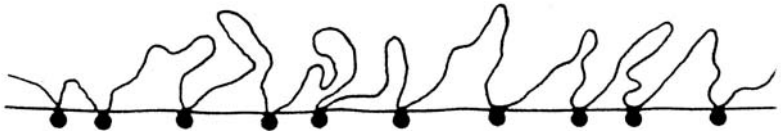

Figure 7. A polymer with widely spaced hydrophilic groups will form irregular loops on water surface.

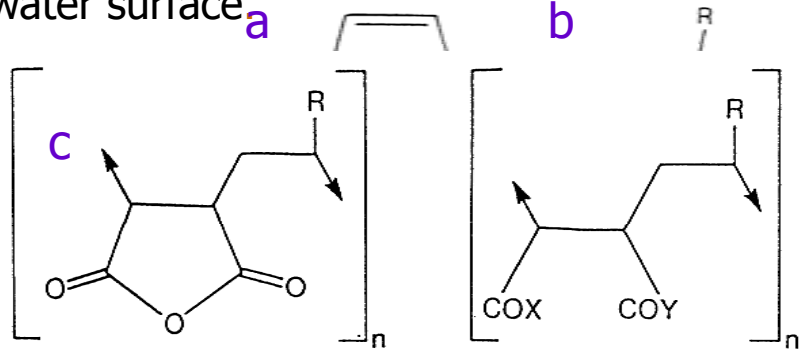

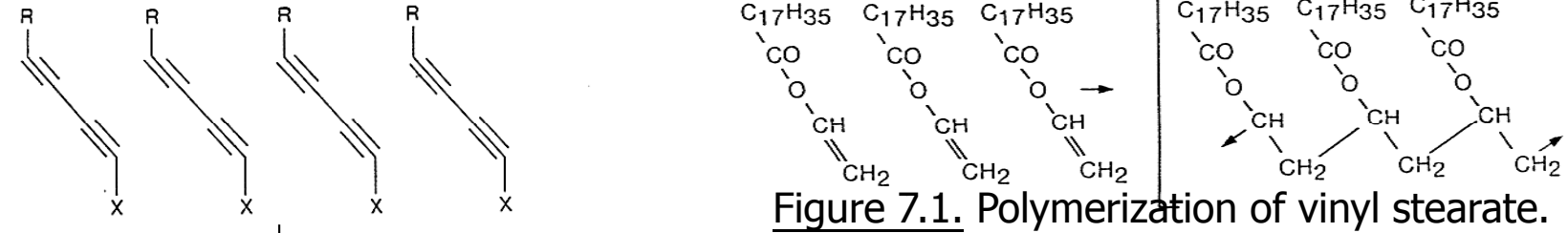

Figure 7.1. Polymerization of vinyl stearate.

Figure 7.2. Polymerization of the oxiran ring.

- Self-assembly is the spontaneous formation of complex hierarchical structure from pre-designed building blocks through non-covalent forces.

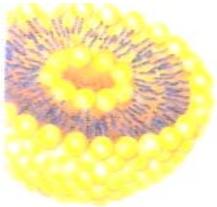

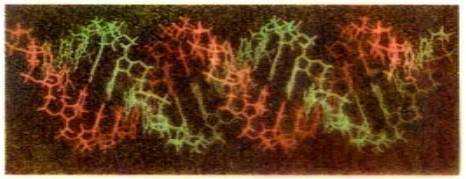

- Self-assembled monolayers (SAMs) are ordered molecular assemblies formed spontaneously on a solid substrate.

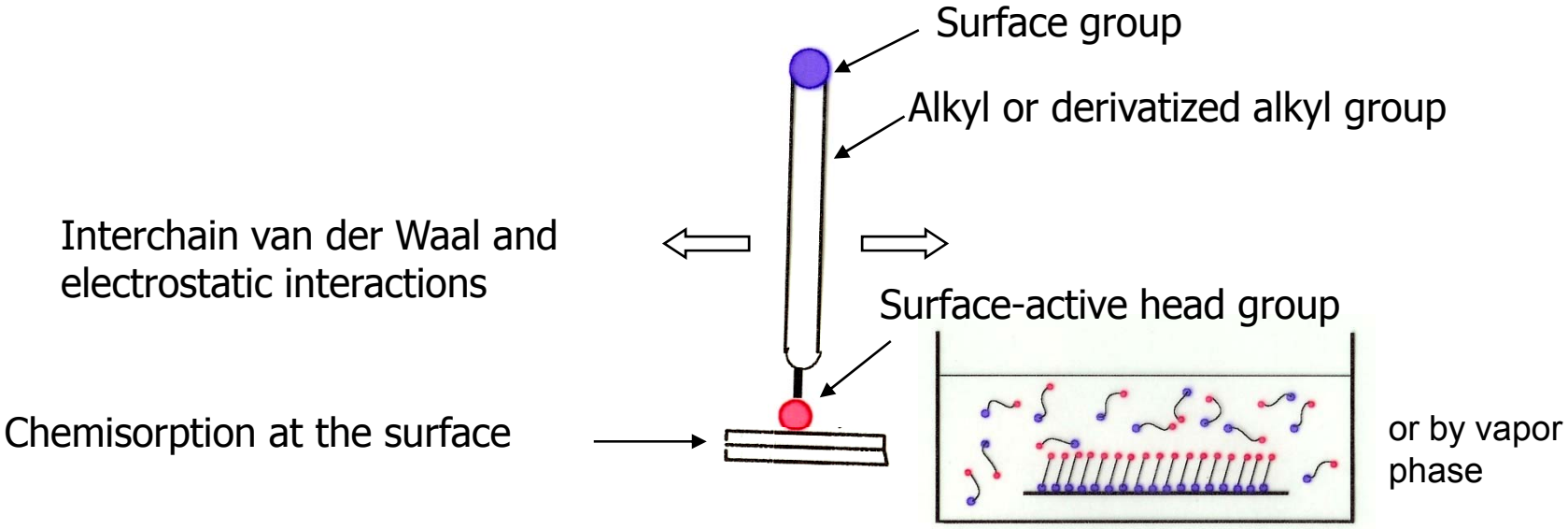

Characterization Techniques

- **Microscopy-based techniques**
  Scanning tunneling microscopy (STM), Atomic force microscopy (AFM).

- **Diffraction-based techniques**
  Low energy electron diffraction (LEED), Grazing-incidence X-ray diffraction (GIXD)

- **Spectroscopy-based techniques**
  IR, SHG, SERS, NEXAFS, XPS…..

- **Other techniques**
  Wetting behavior, ellipsometry, surface plasmon spectroscopy (SPR), QCM, ……

- Advancing contact angles θ_a of water and hexadecane on mono-layers or representative thiols on gold.

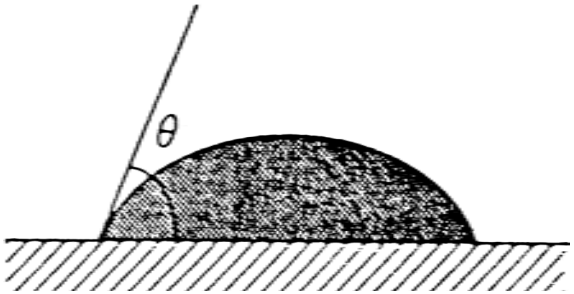

Thiol	Θ_a (H2O) (o)	Θ_a ($C_{16}H_{34}$) (o)	Thiol	Θ_a (H2O) (o)	Θ_a ($C_{16}H_{34}$) (o)
$HS(CH_2)_2(CF_2)_5CF_3$	118	71	$HS(CH_2)_{16}OCH_3$	75	41
$HS(CH_2)_{17}CH_3$	112	47	$HS(CH_2)_{10}CO_2CH_3$	67	28
$HS(CH_2)_{17}CH=CH_2$	107	39	$HS(CH_2)_{11}CN$[b]	63	<5
$HS(CH_2)_{19}Br$[a]	97	<5	$HS(CH_2)_{10}CONH_2$[c]	13	<5
$HS(CH_2)_{14}OCOCF_3$[d]	96	62	$HS(CH_2)_{15}CO_2H$	<10	<5
$HS(CH_2)_{19}F$[a]	95	<5	$HS(CH_2)_{11}OH$	<10	<5
$HS(CH_2)OCH_3$	83	<5			

Infrared Reflection Absorption Spectroscopy (IRRAS)

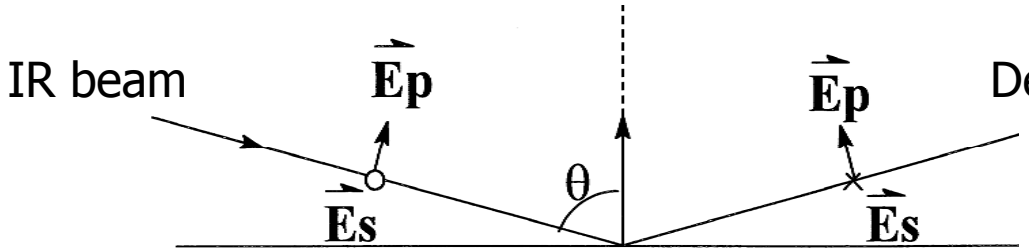

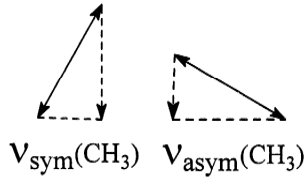

- For Reflective surfaces such as metal:

The vector sum of $\vec{E}s$ at surface approaches 0,

The vector sum of $\vec{E}p$ varies with incidence angle θ

$$I \propto \left| \frac{\partial \vec{\mu}}{\partial q} \cdot \vec{E} \right|^2 \propto \cos^2\alpha = \frac{I_{obs}}{3I_{calc}}$$

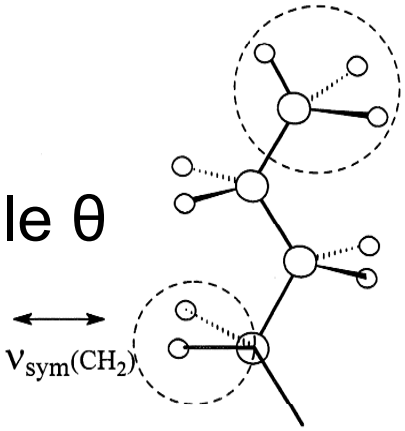

α: angle between $\vec{E}p$ and the direction of transition dipole

Substrates and Ligands that form SAMS.

Substrate	Ligand or Precursor	Binding
Au	RSH, ArSH (thiols)	RS-Au
Au	RSSR' (disulfide)	RS-Au
Au	RSR' (sulfides)	RS-Au
Au	RSO_2H	RSO_2-Au
Au	R_3P	R_3P-Au
Ag	RSH, ArSH	RS-Ag
Cu	RSH, ArSH	RS-Cu
Pd	RSH, ArSH	RS-Pd
Pt	RNC	RNC-Pt
GaAs	RSH	RS-GaAs
InP	$RSiCl_3$,$RSi(OR')_3$	RS-InP

Substrate	Ligand or Precursor	Binding
SiO_2,glass	$RSiCl_3$, $RSi(OR')_3$	Siloxane
Si/Si-H	$(RCOO)_2$ (neat)	R-Si
Si/Si-H	$RCH=CH_2$	RCH_2CH_2Si
Si/Si-Cl	RLi,RMgX	R-Si
Metal oxides	RCOOH	$RCOO^-$ …MO_n
Metal oxides	RCONHOH	RCONHOH …Mo_n
ZrO_2	RPO_3H_2	RPO^{2-}_3…Zr^{IV}
In_2O_3/SnO_2 (ITO)	RPO_3H_2	RPO^{2-}_3…M^{n+}

Proposed structure for n-Alkanoic acid on Silver

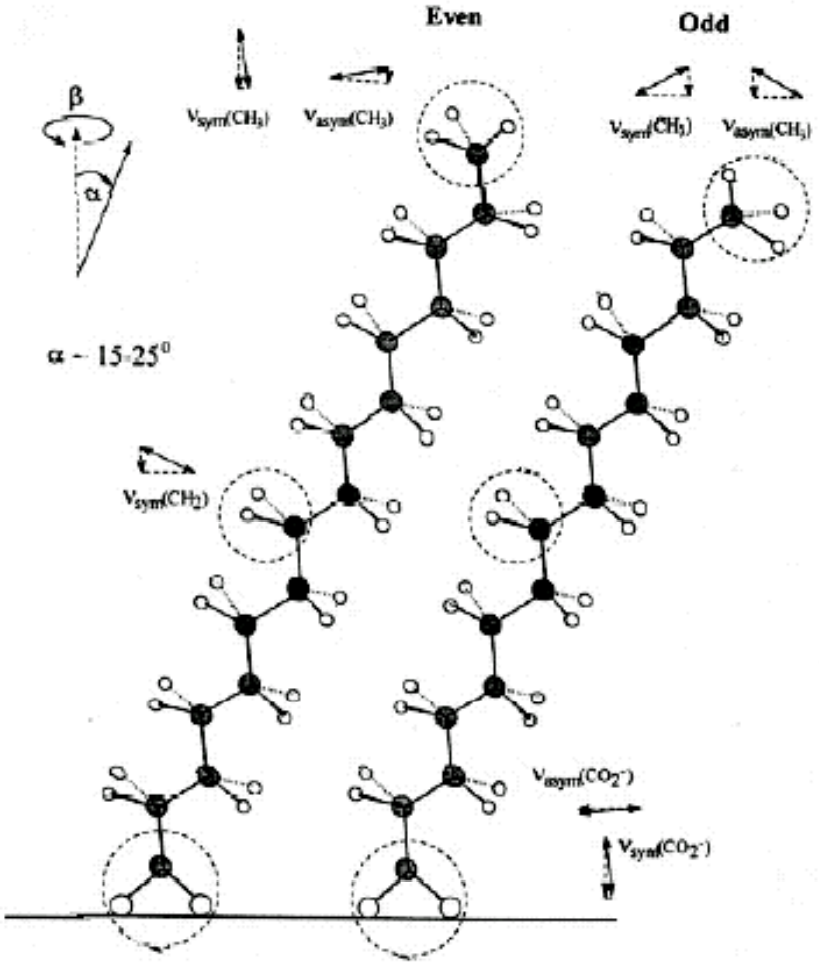

Proposed structure for n-Alkanoic acid on Aluminum and Copper

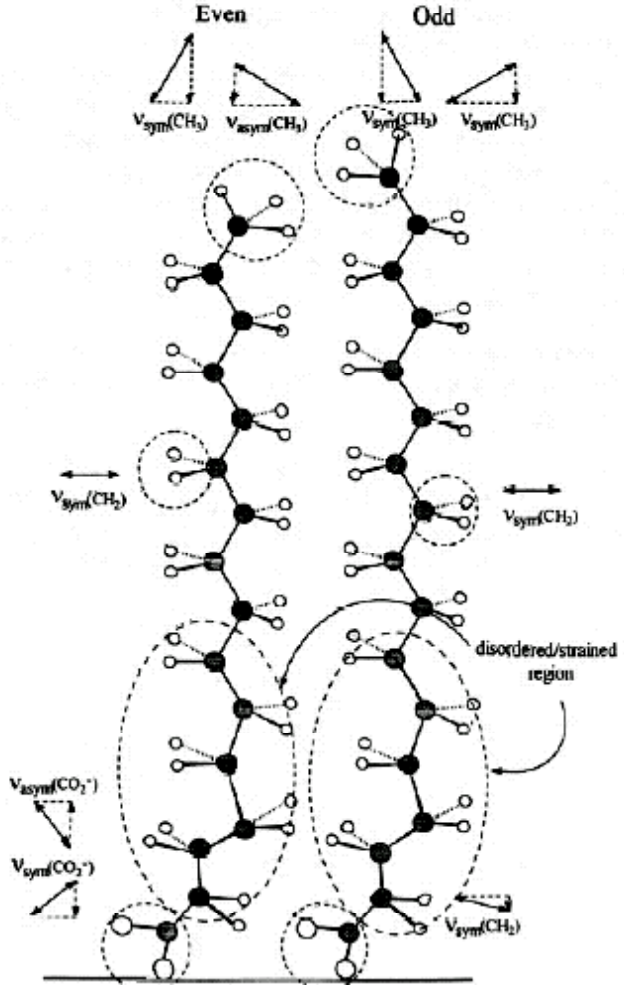

J. Am. Chem. Soc. 1993, V. 115 (10) P. 4356

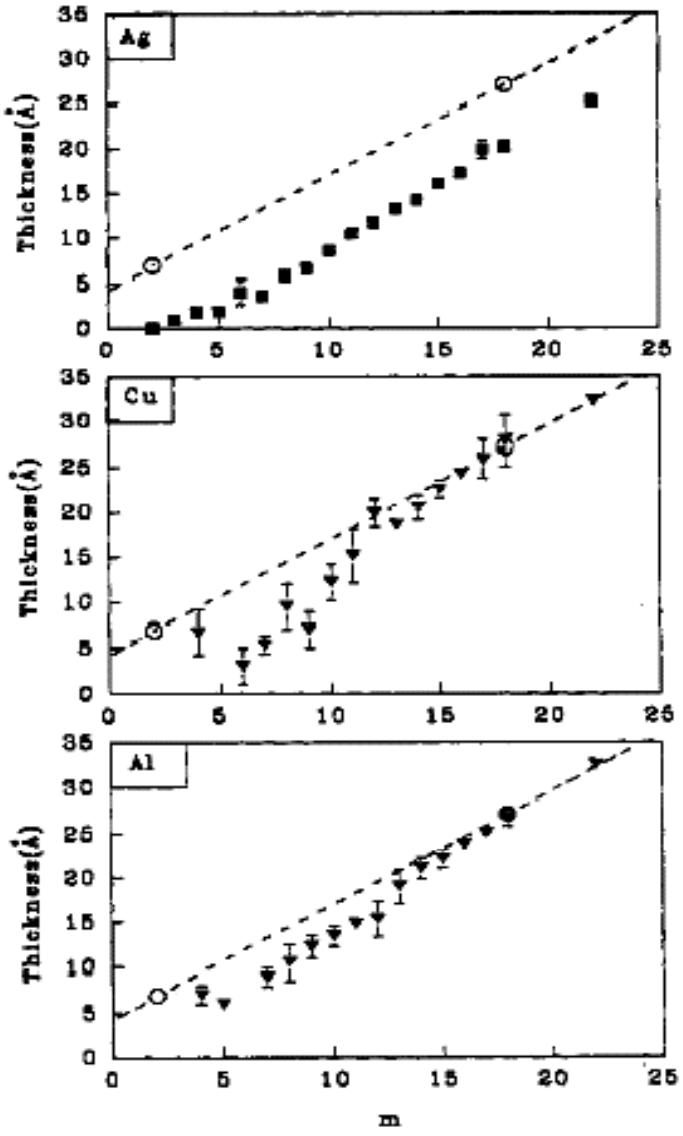

Ellipsometric thickness of the n-alkanoic acid monolayer as a function of chain length. Dashed line represents the calculated thickness for normal orientation.

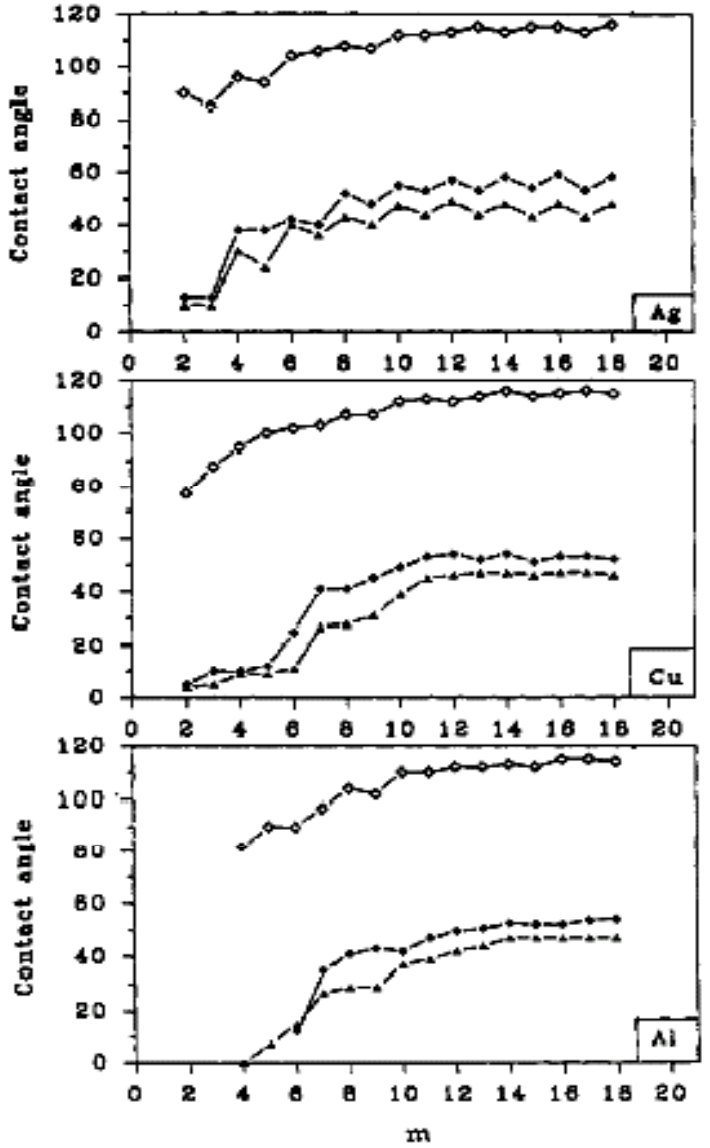

Contact angle on a monolayer surface as a function of chain length of the acid: (Δ)hexadecane, (♦)bicyclohexyl, (◊)water.

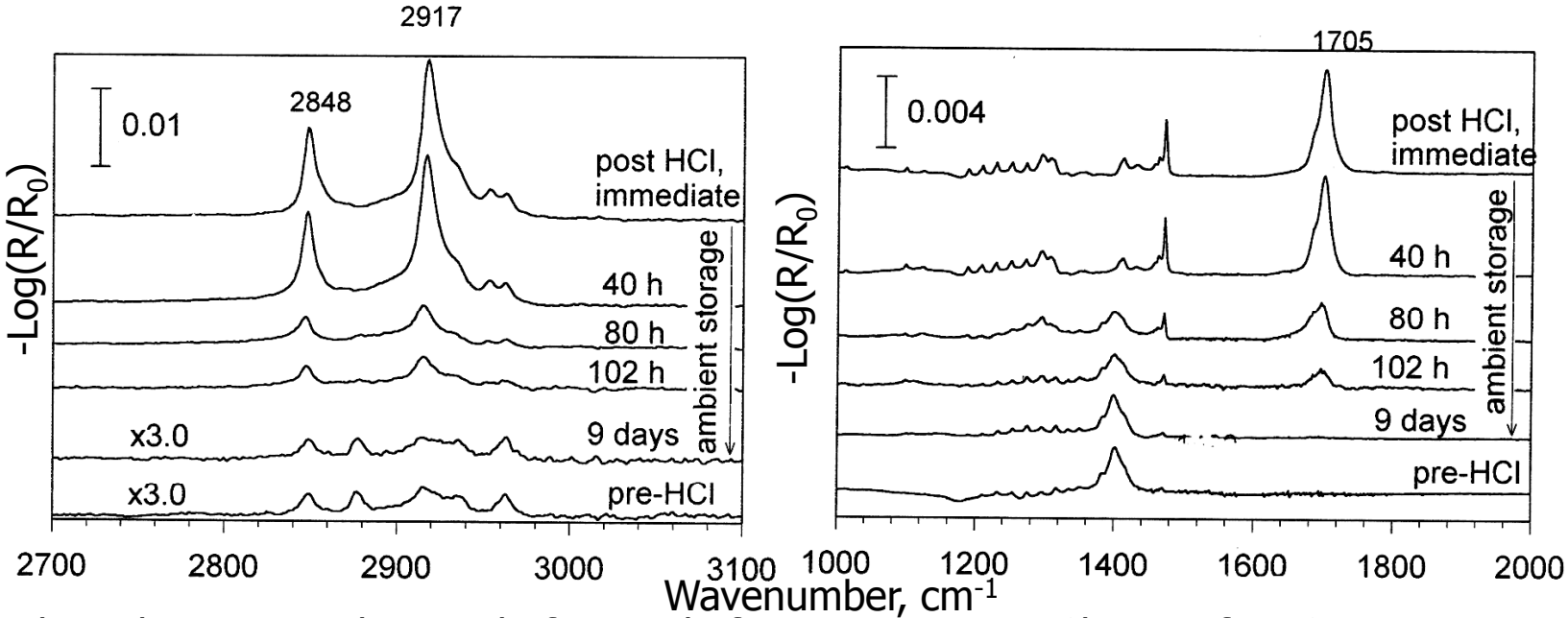

SAM of *n*-hexadecanoic acid on Ag before and after exposure to HCl vapor for 10 sec.

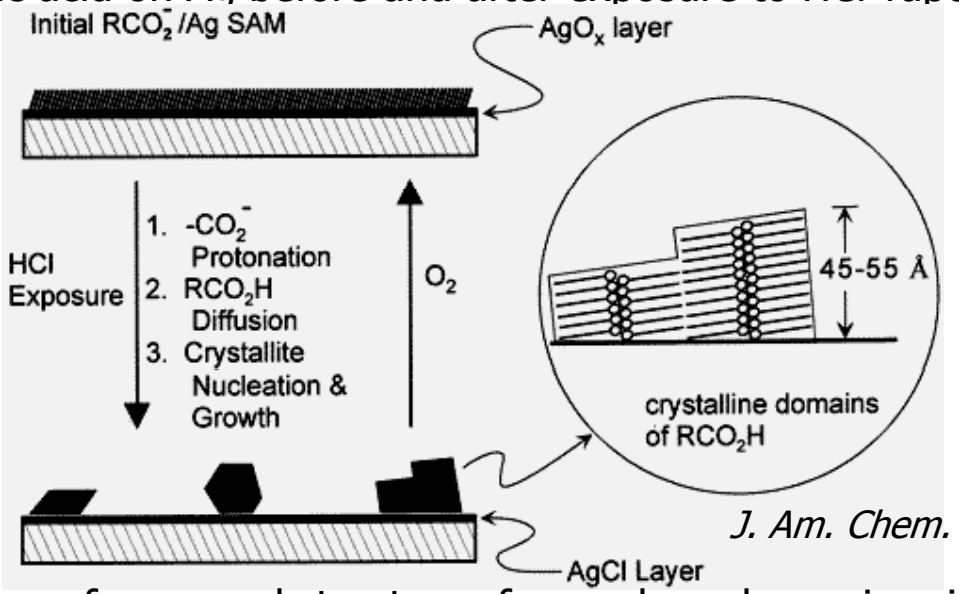

J. Am. Chem. Soc. 1996, V. 118 (28) P. 6724

Schematic representation of proposed structures for a *n*-hexadecanoic acid monolayer on Ag before and immediately after a 10-s HCl exposure.

General Reaction Mechanism

- RCO_2^-(2-D,c)/M[oxide]/M + HCl(g) ---> RCO_2H*(2-D,c)/M[Cl^-]/M
- RCO_2H*(2-D,c)/M[Cl^-]/M---------- > RCO_2H*(3-D,c)/M[Cl^-]/M
- RCO_2H*(3-D,c)/M[Cl^-]/M + O_2(g) ---- > RCO_2H*(3-D,c) / [oxide] /M
- RCO_2H*(3-D,c)/M[oxide]/M ----------> RCO_2^-(2-D,c)/M[oxide]/M

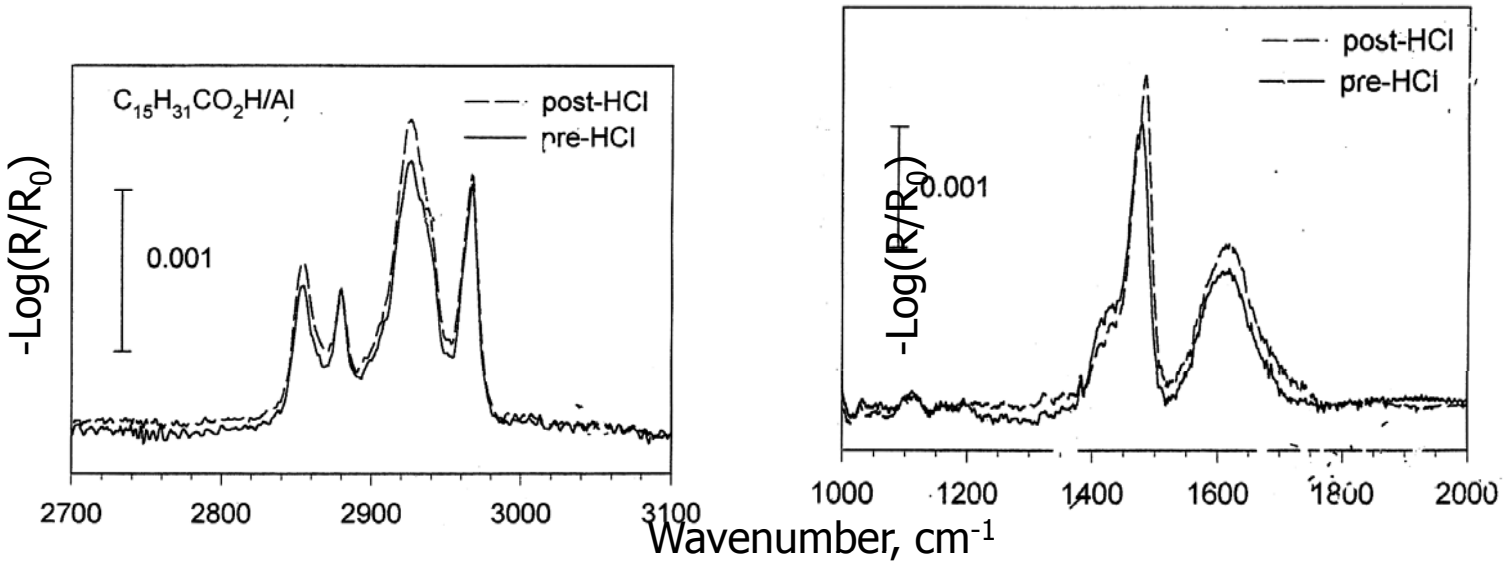

n-hexadecanoic acid monolayer on Al before and after HCl exposure

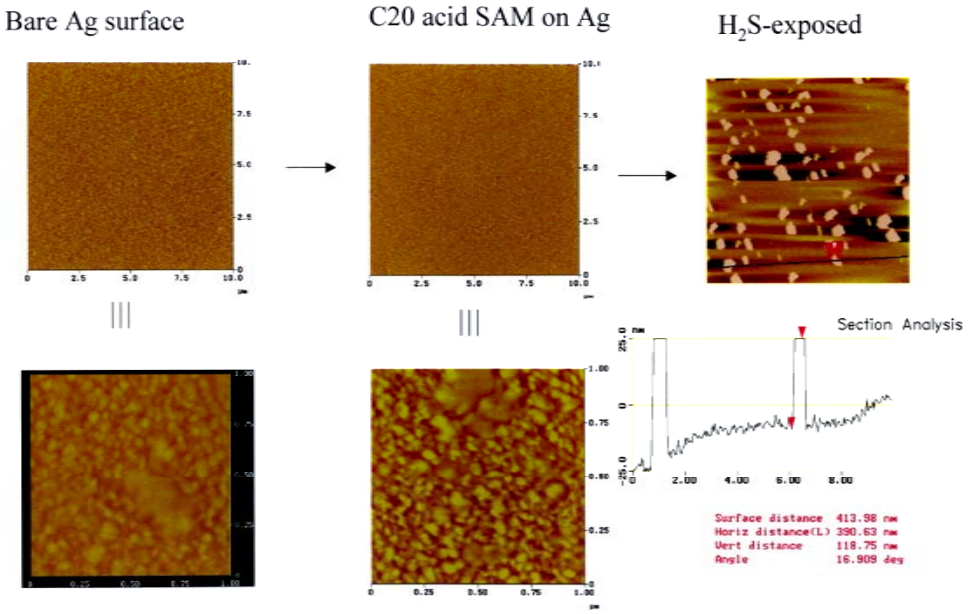

Restoration of monolayer of eicosanoic acid on Ag surface at 38°C, completed in 90 min.

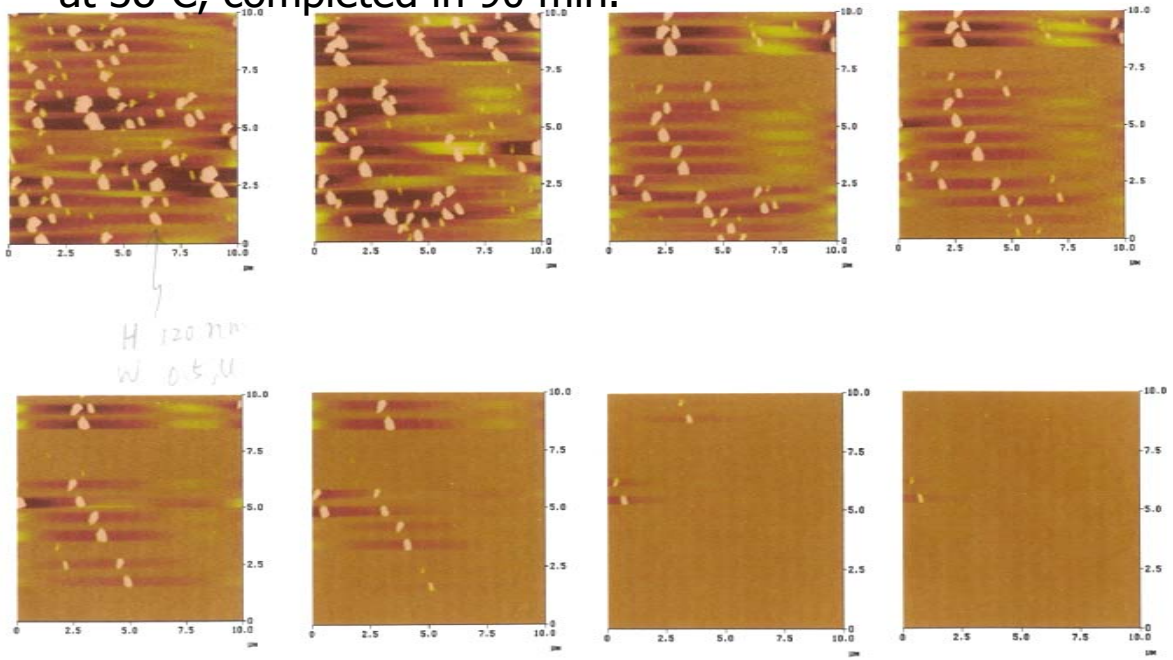

Adsorption of Alkyltrichlorosilane on Hydroxylated Surfaces

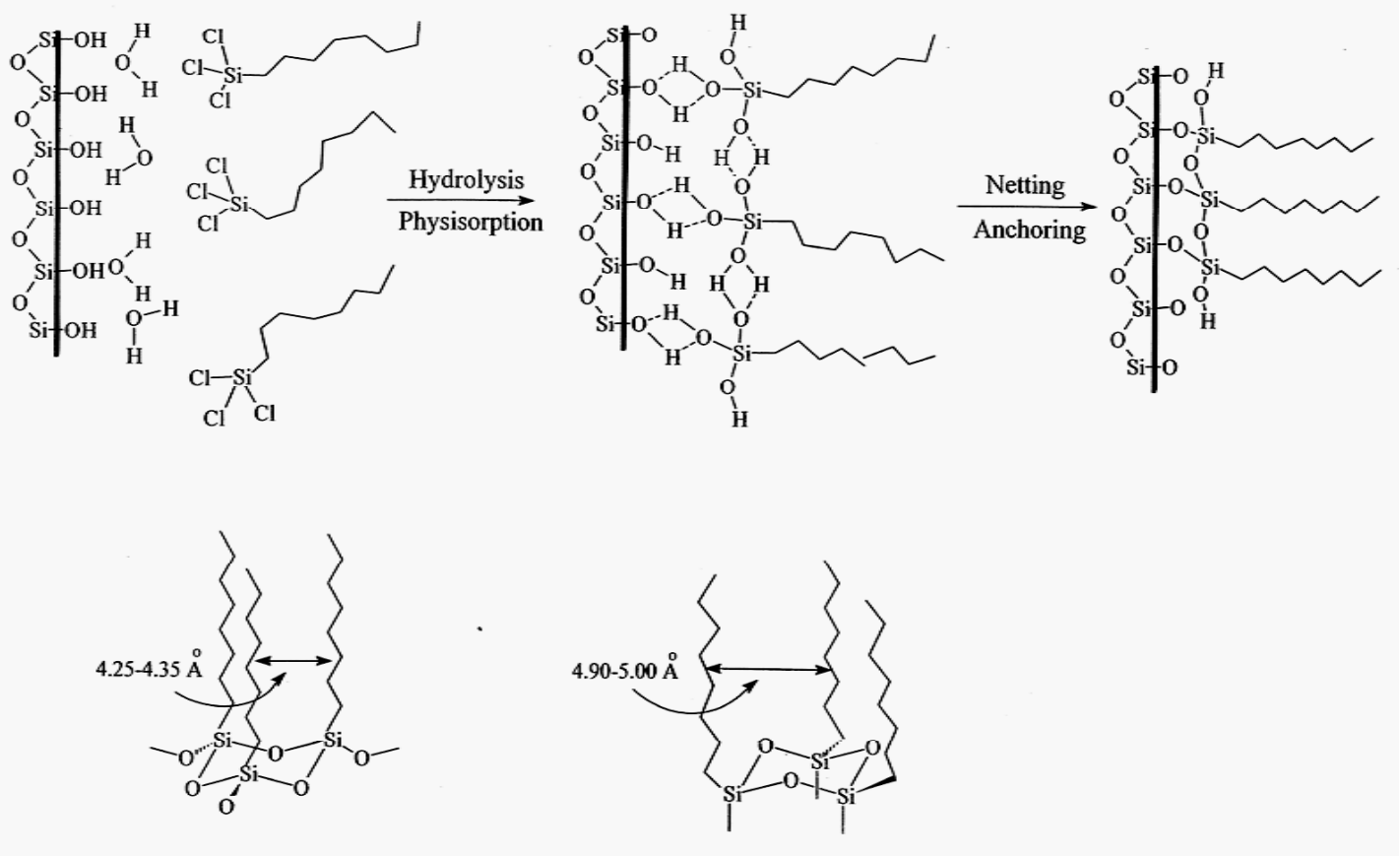

substrates: SiO_2, glass, Al_2O_3, quartz, mica….
silanes: trichlorosilane, trimethoxysilane, triethoxysilane…

Alkanethiol on gold surfaces

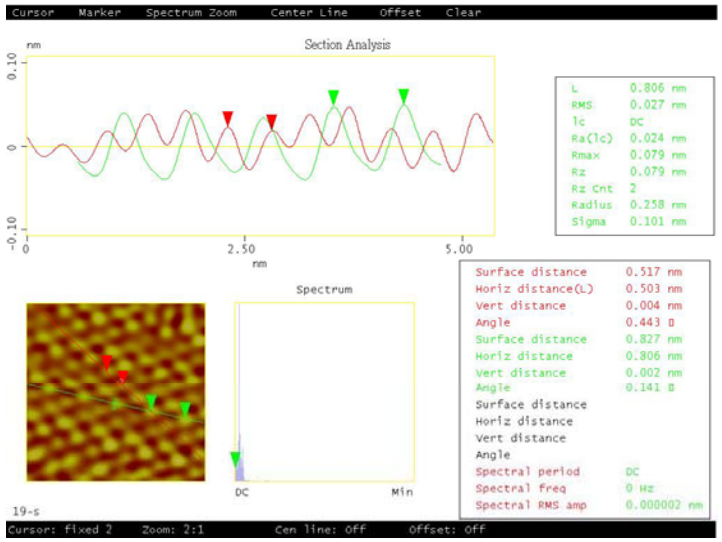

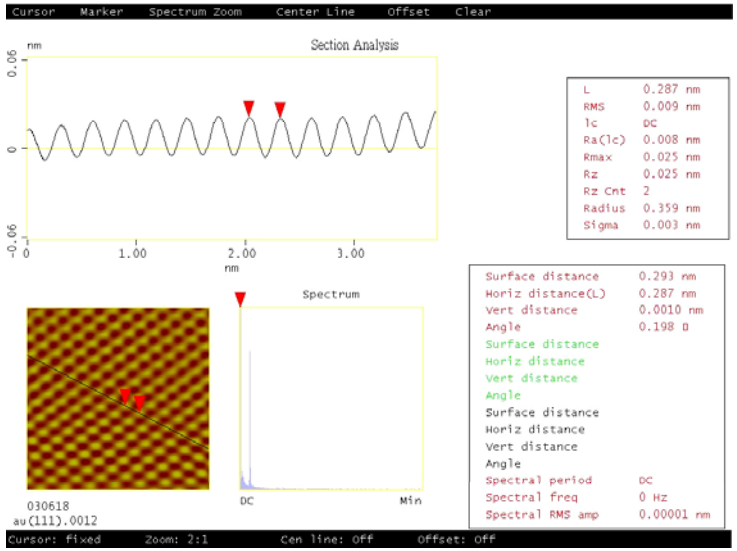

$$RSH + Au^{o}_{n} \rightarrow RS^{-}Au^{+}\bullet Au^{o}_{n-1} + \tfrac{1}{2} H_2$$

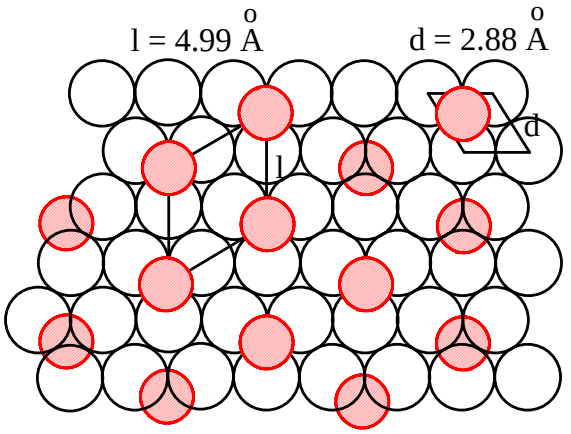

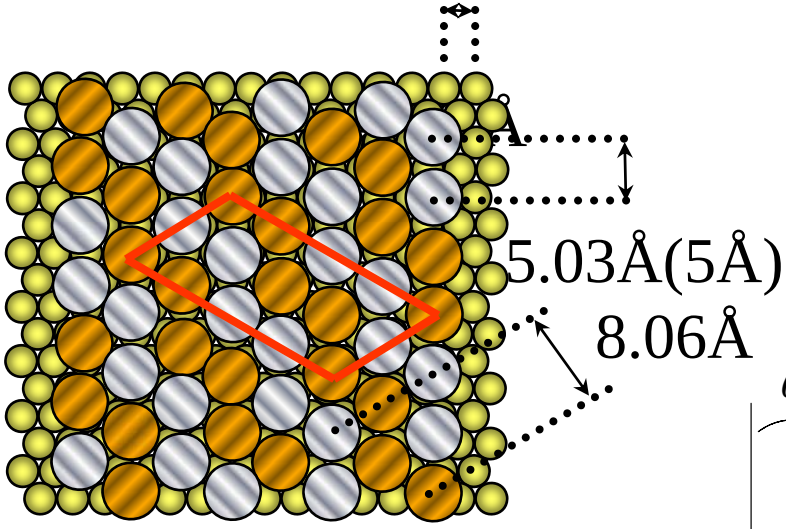

binding scheme for sulfur atoms

$(\sqrt{3} \times \sqrt{3})$ R30°

top surface superlattice: C(4X2)

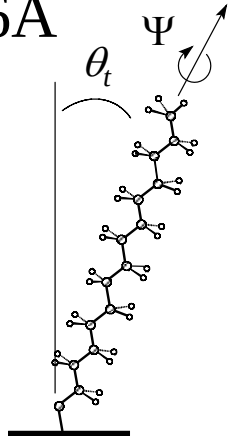

Other thiols forming self-assembled monolayer:

***n*-Alkenethiols**

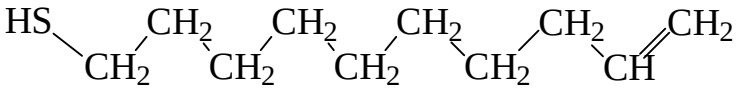

OH-terminated thiols

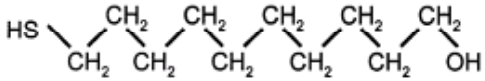

COOH-terminated thiols

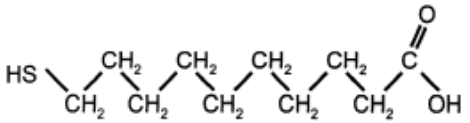

Oligophenylthiols

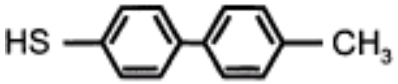

Fluorinated alkanethiols

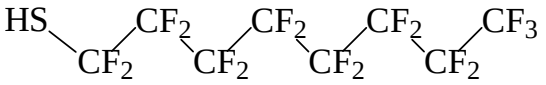

Dialkyl disulfides and dialkyl sulfides

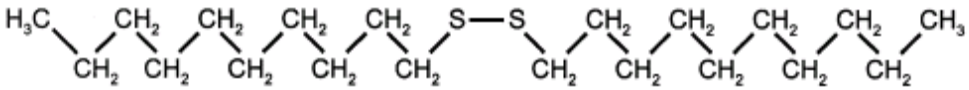

Dithiols

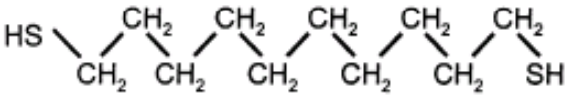

Structure of $PhPhCH_2SH$ SAMs

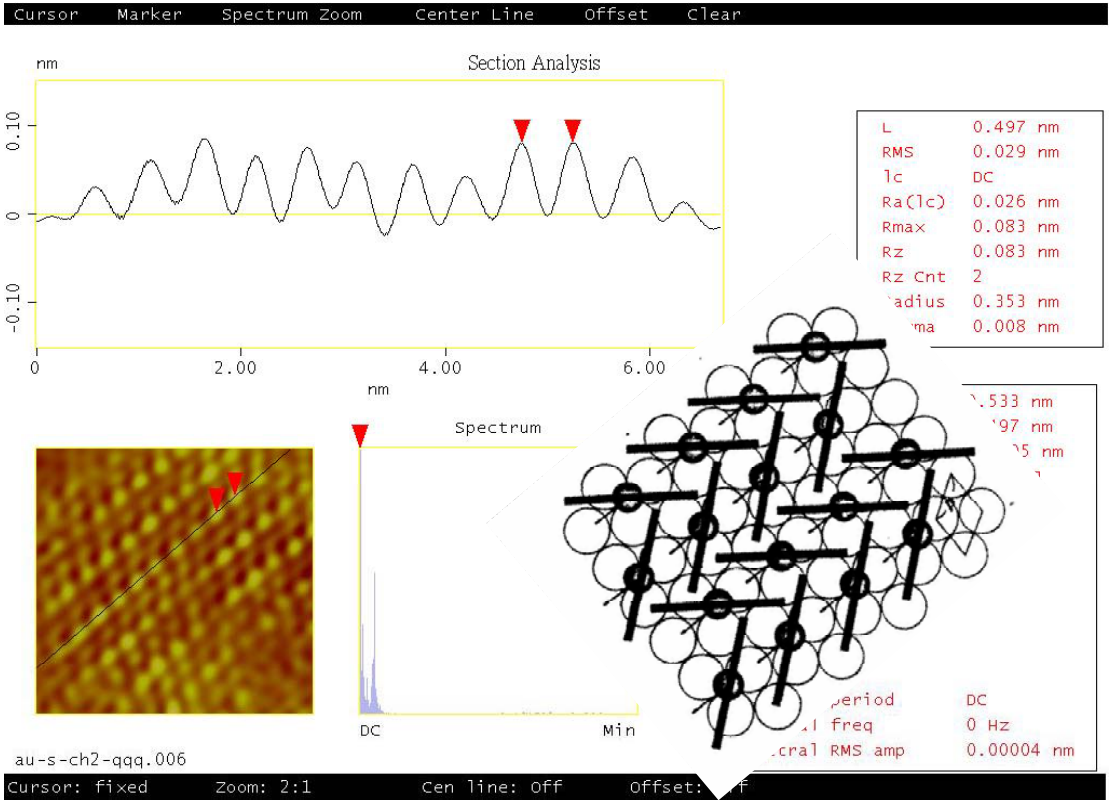

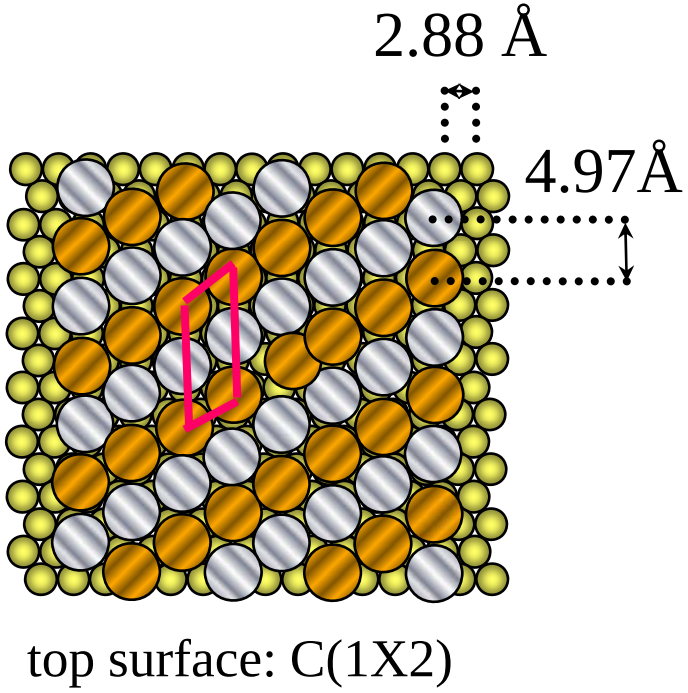

top surface: C(1X2)

- The packing density (x10^{-10}mol/cm^2) and the desorption potential (mV) in parenthesis of aromatic-derivatized thiols on evaporated Au using electro-chemically reductive desorption method.

X=	I	II	III	IV
H	4.4+0.4(-848)	8.1+0.3(-921)	6.1+0.7(-926)	8.0+0.3(-1091)
OCH_3	5.1+0.3(-921)	8.1+0.3(-939)	5.2+0.8(-907)	8.0+0.1(-1087)
$OC_{16}H_{33}$	6.3+0.6(-1215)	8.0+0.4(-1182)	7.8+0.3(-1305)	7.5+0.3(-1197)

$Au\text{-}S\text{-}C_{16}H_{33}$ 7.8+0.1(-1130)

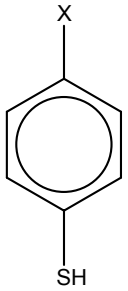

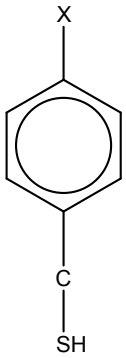

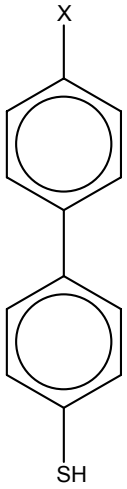

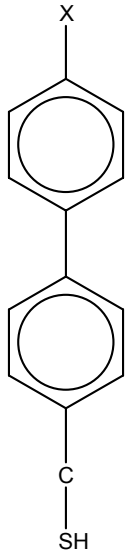

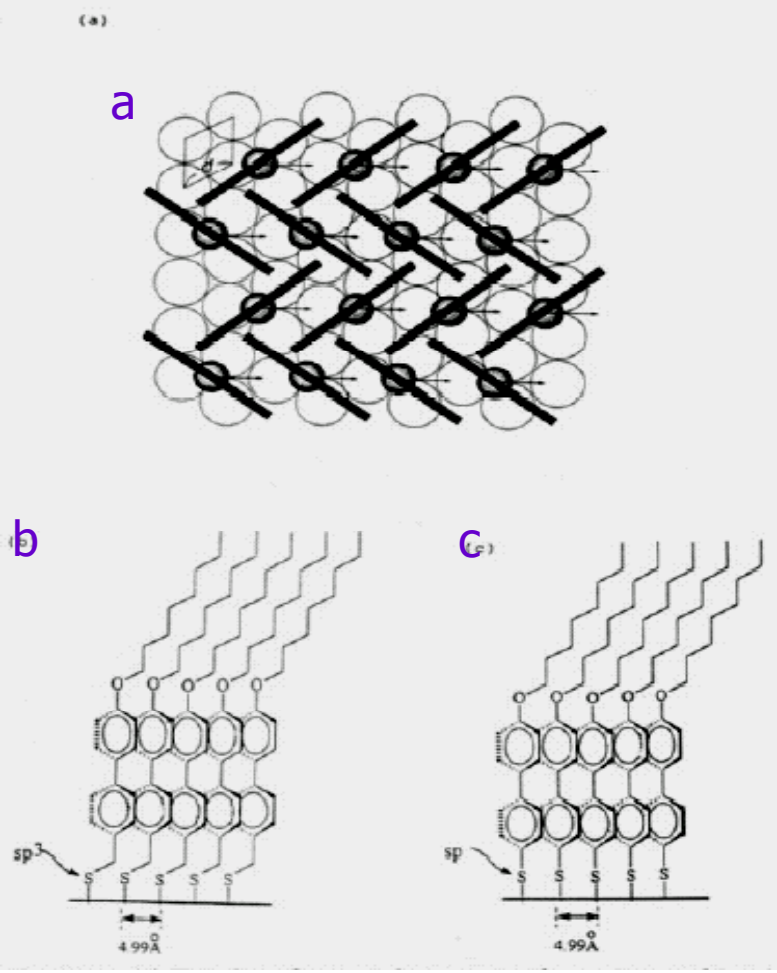

(a) Top view of proposed structures of monolayers of I and III on the (√3*√3) R30° overlayers of Au(111) and Ag(111) surfaces. The arrow indicates the tilting direction of alkyl chain. (b) Side view of monolayer of I along a line connecting the nearest neighbors. (c) Side view of monolayer of III.

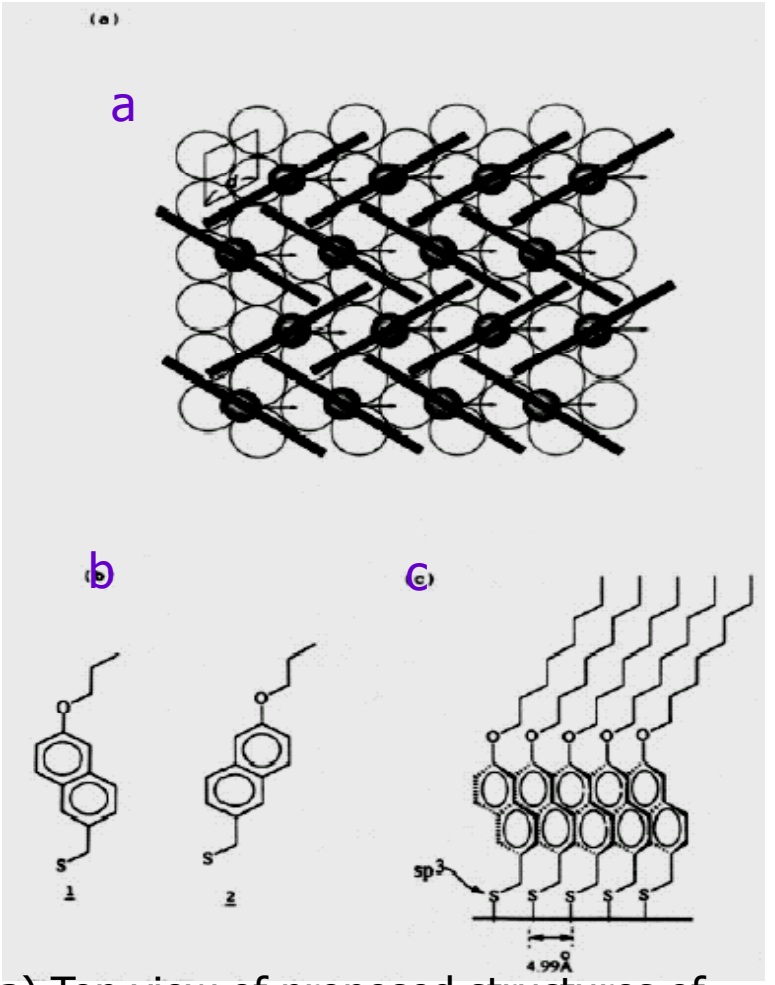

(a) Top view of proposed structures of monolayers of II on the (√3*√3)R30° overlayers of Au(111) and Ag(111) surfaces. The arrow indicates the tilting direction of alkyl chain. (b) Four confirmations for head group. (c) Side view of monolayer along a line connecting the nearest neighbors.

Fluorinated alkanethiol

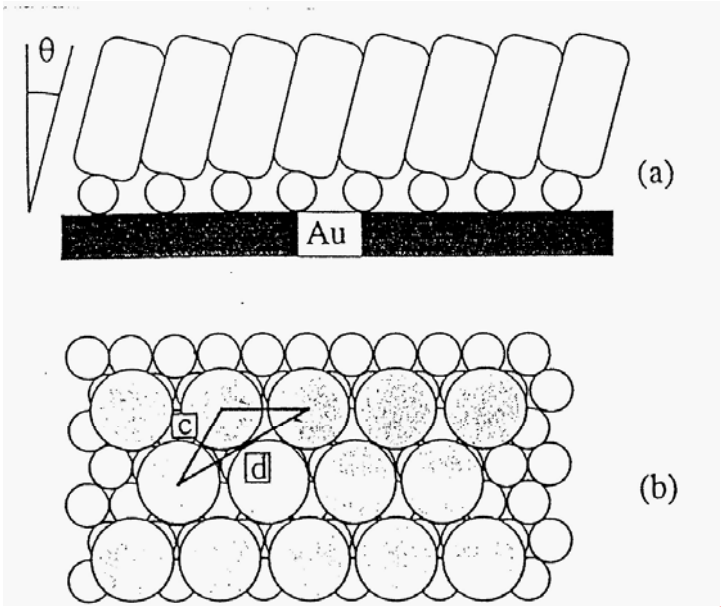

- Schematic illustration of the idealized structure for the monolayer formed from the chemisorption of $CF_3(CF_2)_7(CH_2)2SH$ at Au(111). The tilt(θ) of the perfluorocarbon chains in the side view (A) is 16o with respect to the surface normal. The corresponding (2*2) adlayer structure is depicted in the top view (B). The spacings between adsorbates is 0.58 nm (c) and 1.0 nm (d)

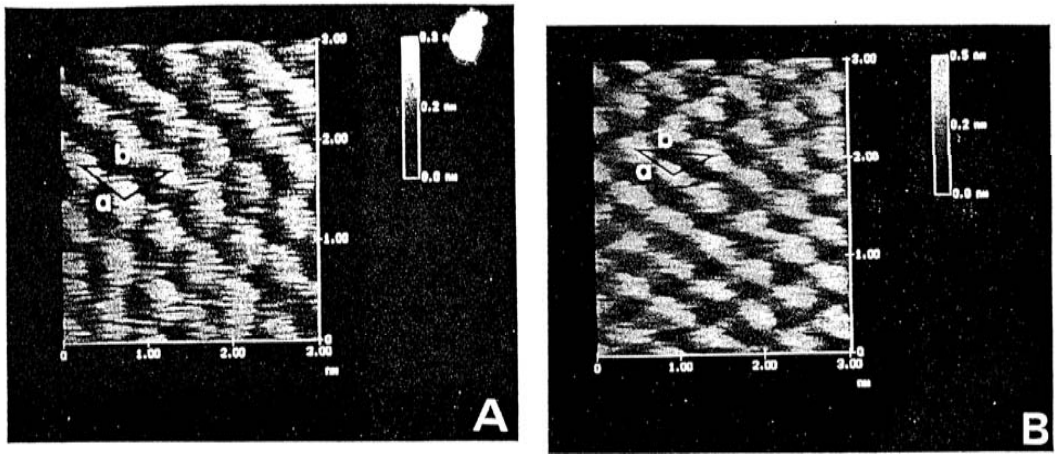

- (A) An AFM image covering 3.0nm*3.0nm of $CF_3(CF_2)_7(CH_2)2SH$ chemisorbed at Au(111). The nearest-neighbor and next-nearest-neighbor spacings are 0.58±0.02 and 1.01±0.02 nm, respectively, (B) An AFM image covering 3.0nm*3.0 nm of decanethiolate at Au(111). The nearest-neighbor and next-nearest-neighbor spacings are 0.50±0.02 and 0.91±0.04 nm, respectively.

J. Am. Chem. Soc. 1992, V. 114 (4) P. 1224

For dithiols, conflicting results obtained. Both “standing-up” phases and “lying-down” phases have been reported.

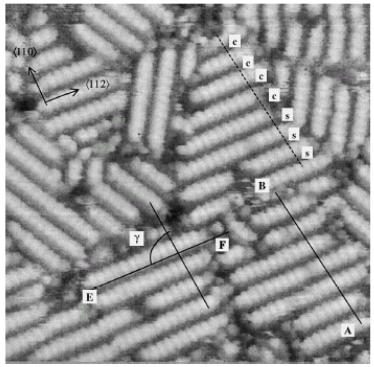

Fig. 10. Constant-current STM image (220 Å × 220 Å) of 1,6-hexanedithiol on Au(1 1 1) prepared at room temperature by gas phase deposition. Periodicities along the two lines AB and EF (inclining an angle, γ, of 95°) are 13.3 and 5 Å. Note that bright features are meandering as explained in text. From [130].

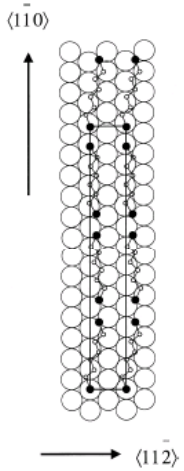

Lying-down configuation

GIXD, LEAD, STM, Langmuir, 16, (2000), 549.

STM, IR, Jpn. J. Appl. Phys. 37, (1998), L297.

Standing-up configuration

XPS, IR, Ellipsometry, J. Am. Chem. Soc. 117, (1995), 9529.
XPS, Langmuir, 14, (1998), 5147.

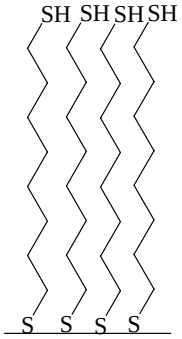

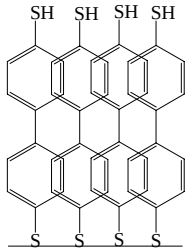

For long chain or rigid-rod α,ω-dithiols, standing-up phase is energetically most favorable configuration.

Alkanethiol on silver surfaces

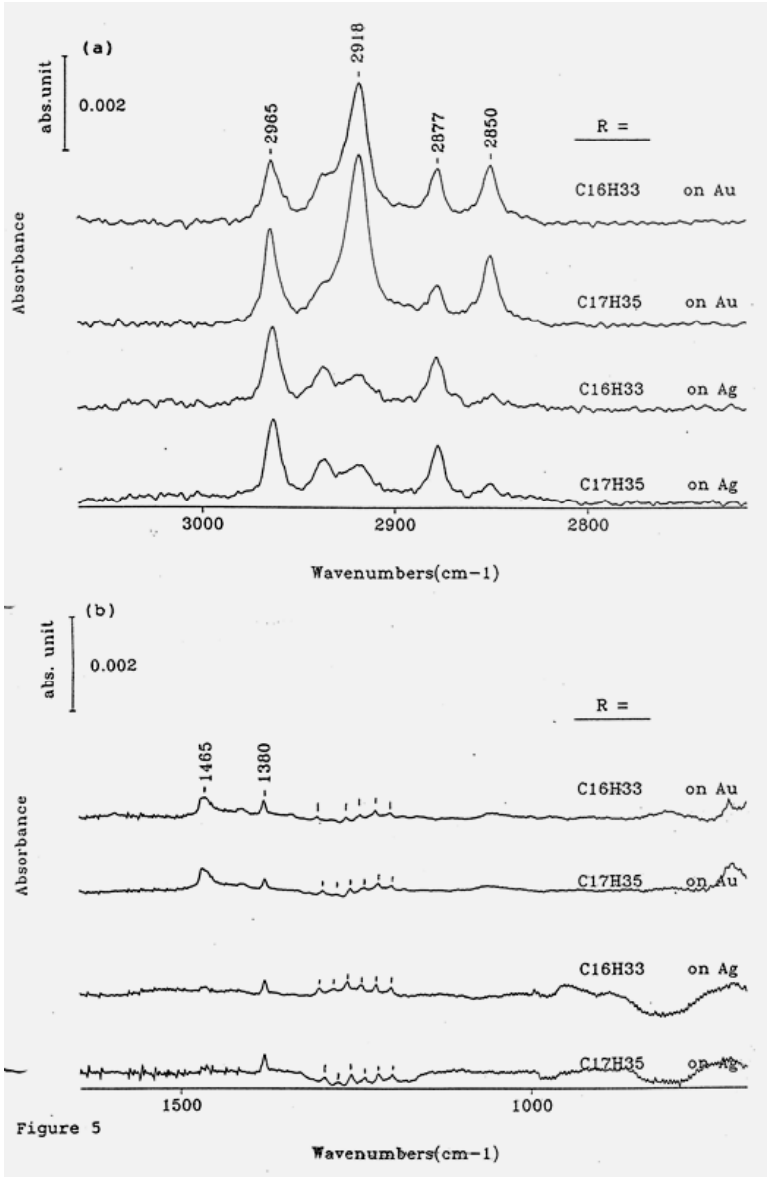

Figure 5

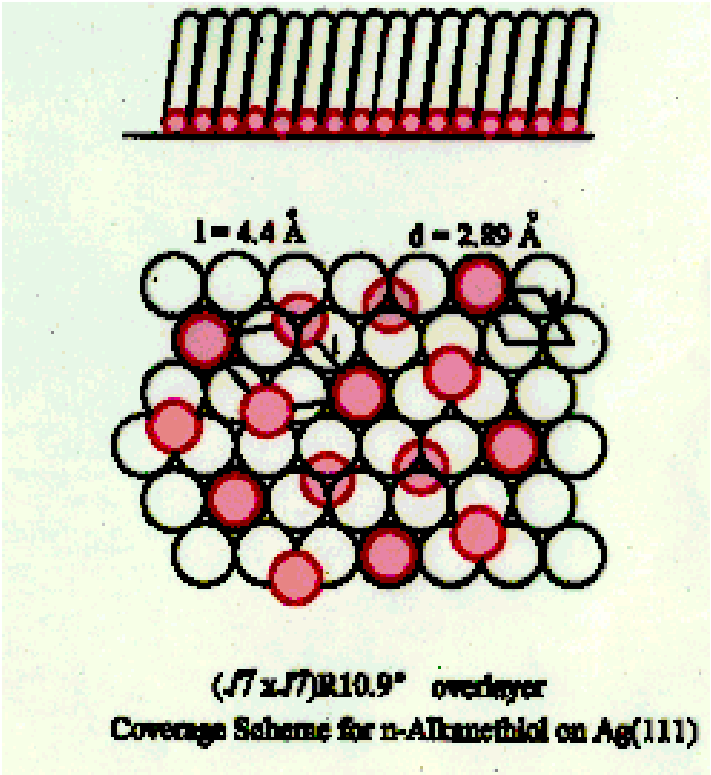

incommensurate with Ag(111),
lower tilt (~13°), higher molecular coverage

Why Alkanethiolate SAMs on Au(111) and Ag(111) are Different?

1 X 3 assembly at 4.2-Å spacing (left), representing alkanethiolate on Ag(111), and at 4.97 Å-spacing (right), representing alkanethiolate on Au(111).

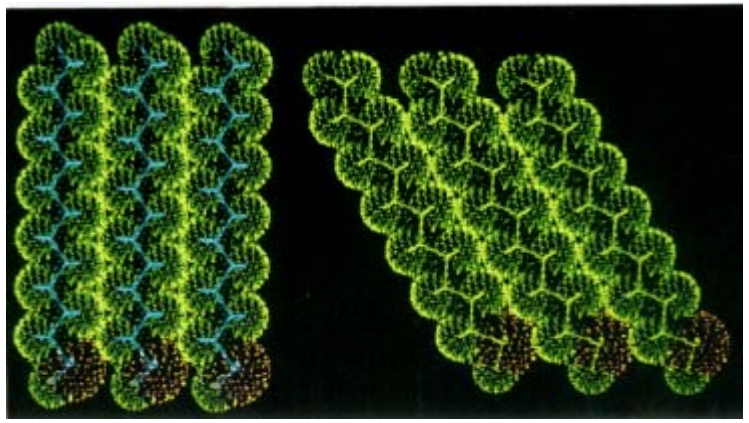

Best interaction energy (for optimal in-plane tilt) *as* a function of the spacing (d).

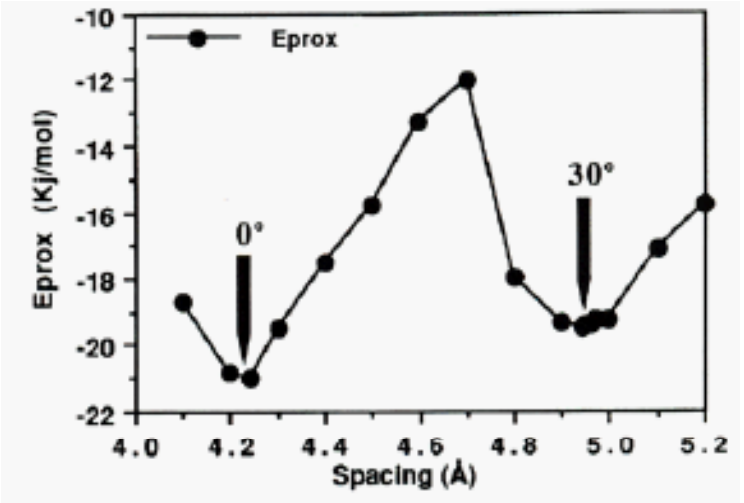

Ulman, A.; Eilers, J. E.; Tillman, N. *Langmuir*, 1989, *5,* 1147

Why are Alkanethiolates on Au(111) and Ag(111) Different?

Facts:

1. **The nearest-neighbor distance for Au(111) and Ag(111) lattices are similar (2.88 and 2.89 Å, respectively.)**
2. **Iodine forms a $(\sqrt{3}\times\sqrt{3})R30^{o}$ structure on Ag(111), with the iodine atoms occupying the hollow sites.**

Difference between of alkanethiolate SAMs on Au(111) and on Ag(111) must result from an interplay of chemisorption and chain-chain interactions:

1. **Silver is more reactive than gold, it forms an oxide spontaneously, its oxidation potential is 1.7 eV lower, and its work function 0.6 eV lower.**
2. **Gold and silver differs due to relativistic effects. The peak-to-valley roughness at their [111] lattices, 6.0 kcal mol^{-1} for Au(111) and only 3.3 kcal mol^{-1} for Ag(111). Site selection is more effective for Au(111).**

Why are Alkanethiolates on Au(111) and Ag(111) Different? - *Continued*

3. **Because in Ag(111) the energy difference is smaller than in Au(111), adsorption at an on-top site in the former may compete with that at the hollow site.**
4. **Only certain combinations of chain-chain separation and tilt angles permit truly effective packing of alkyl chains. The most effective packing is a trigonal lattice with spacing near 4.4 Å with a molecular axis normal to the surface. This distance (4.41 Å) was found for methanethiolate on Ag(111); however, for longer alkyl chains the distance of 4.6 Å has been reported. The second most effective has a spacing near 5.0 Å and the molecular axis tilted 30º, such that the distance between the chains is, again, 4.4 Å and the fit of bulges into depressions is again perfect.**
5. **Crowding more molecules per unit surface area will result in both more chemisorption energy and VDW attraction for the entire system simply because there are more chains involved. This is a lot of energy, since the possibility of adsorption at on-top sites means that in SAMs of thiolates on Ag(111) there are 26% more chains per unit area than on Au(111) on-top sites.**

Thiols on other surfaces

Thiols on Cu, densely packed monolayer with Low chain tilt (~12°)

Thiols on GaAs(100), densely packed monolayer with higher chain tilt,

Thiols on mercury, a intermediate between Langmuir films and SAMs,

Mixed Monolayer System

By coadsorption

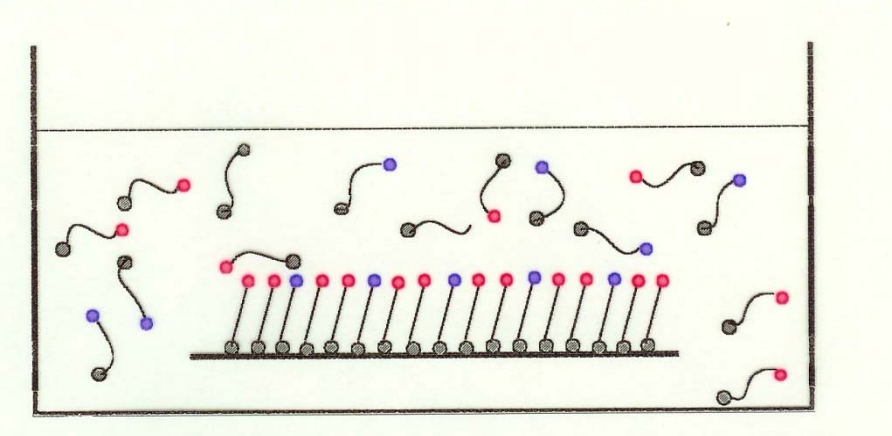

Adsorption from a mixture of components 1 and 2.

By exchange

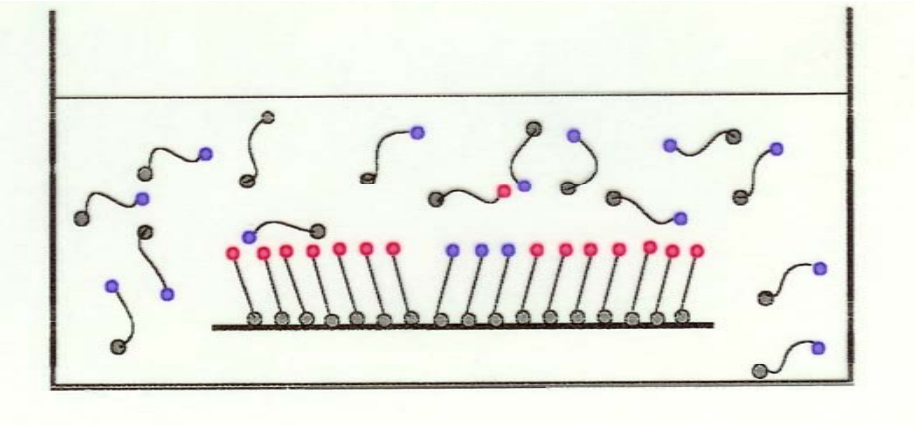

A preformed monolayer of component 1 dipped in a solution of component 2.

Structure of Mixed Monolayer

Type A: Two components with same chain length

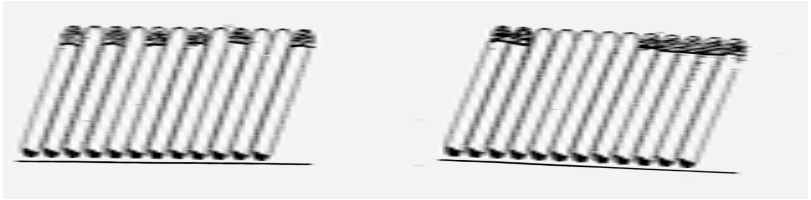

Type B: Two components with different chain length

(1) Longer polar component

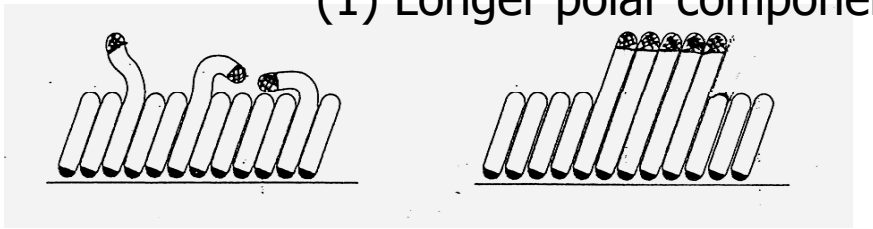

(2) Shorter polar component

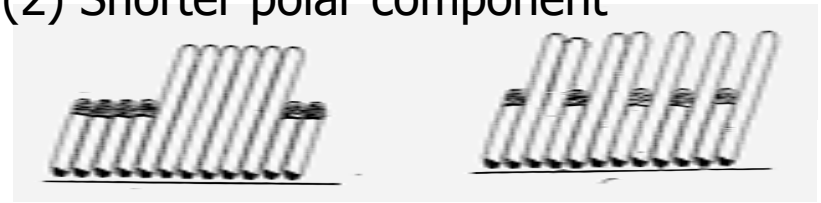

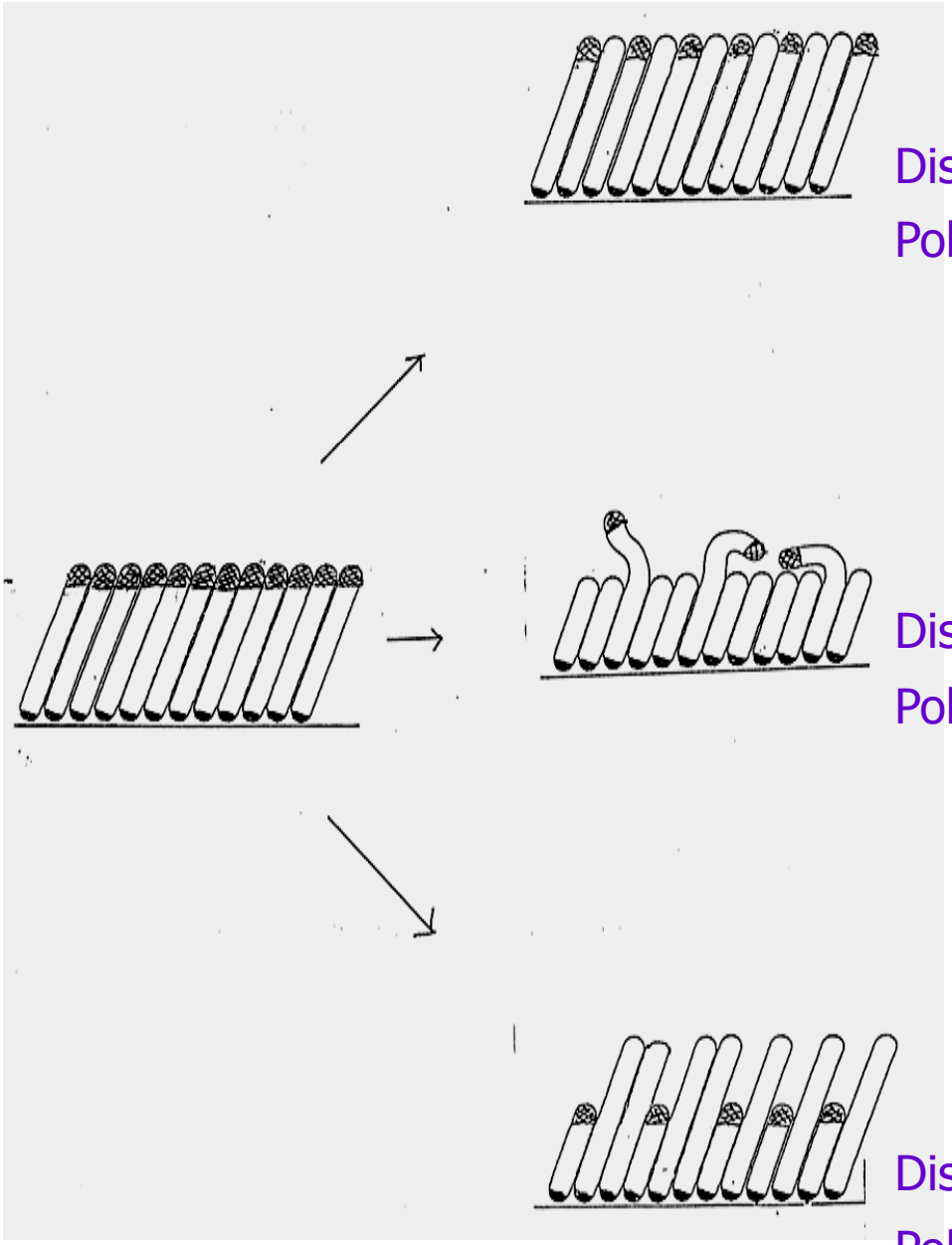

Dispersive interaction

Polar interaction

Dispersive interaction

Polar interaction

Dispersive interaction

Polar interaction

Two sequential scanning tunneling microscope images showing a 500*310 Å^2 area of a self-assembled monolayer os a mixture of 25% $CH_3(CH_2)_{15}SH$ and 75% $CH_3O_2C(CH_2)_{15}SH$ on Au. The color scale and tunneling conditions are the same as in previous slide. The right image was recorded 37 min. after the left image. Two arrows indicate regions where methyl- and methyl ester-terminated thiolate molecules have exchanged, leading to coalescence of domain of methyl-terminated thiolate molecules.

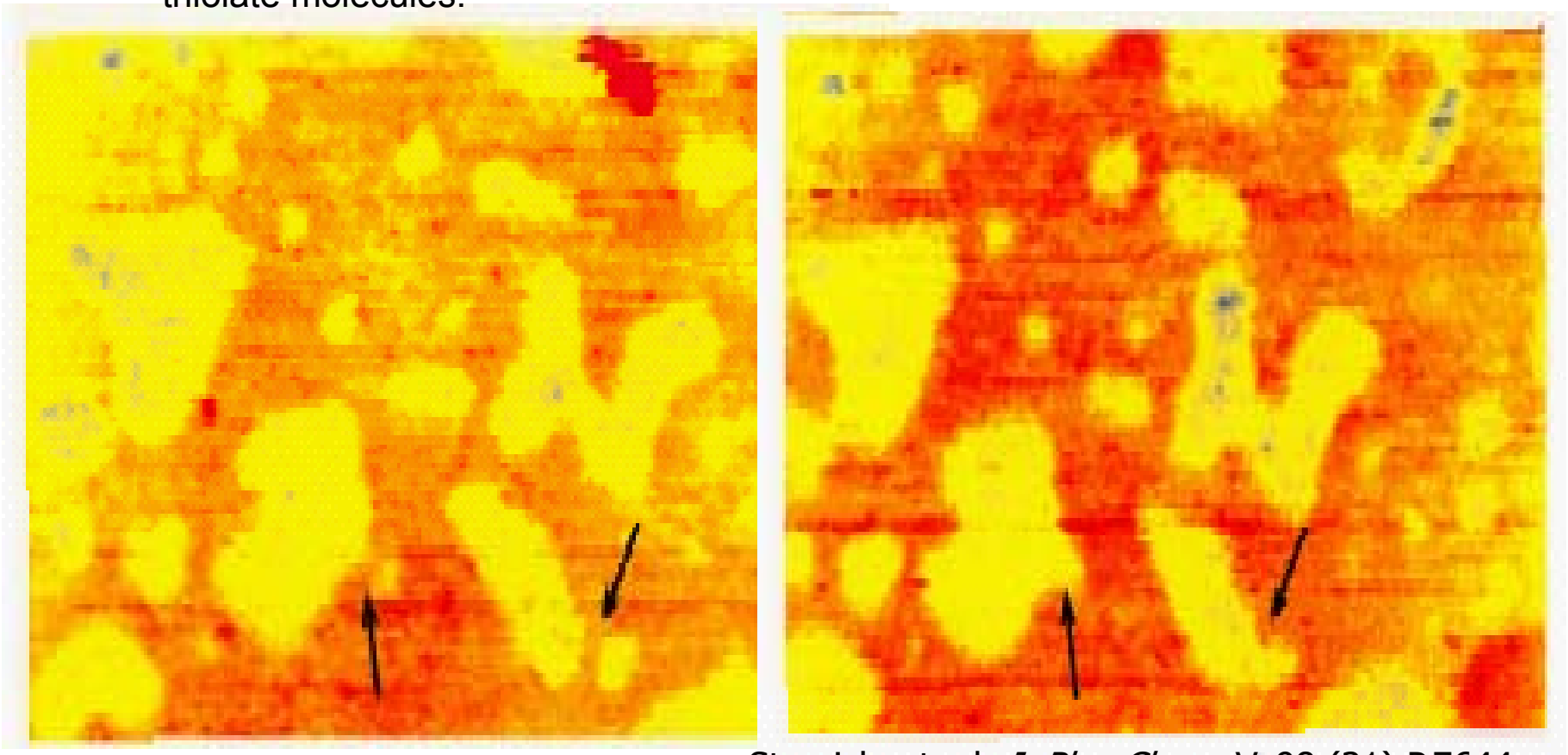

Stranick, et. al. *J. Phy. Chem*. V. 98 (31) P.7644

Multilayer Formation with Polar Order

Sagiv's Approach

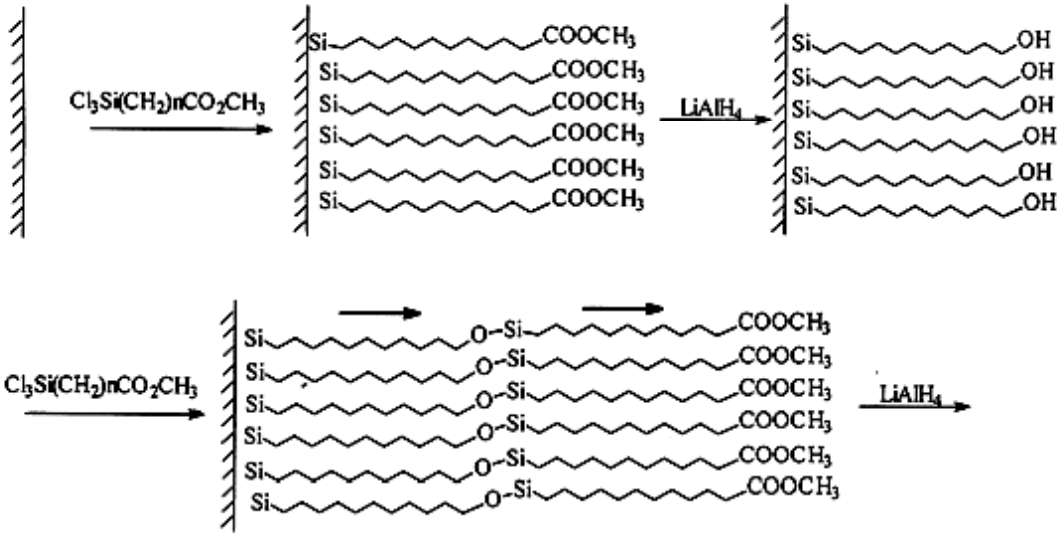

Mallouk's Approach

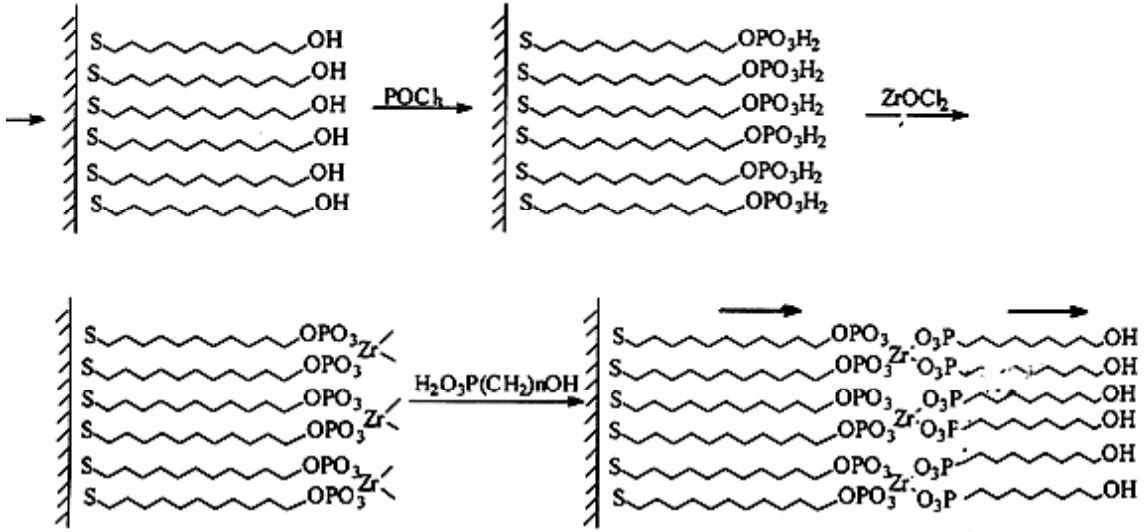

Monolayer Protected Clusters (MPC)

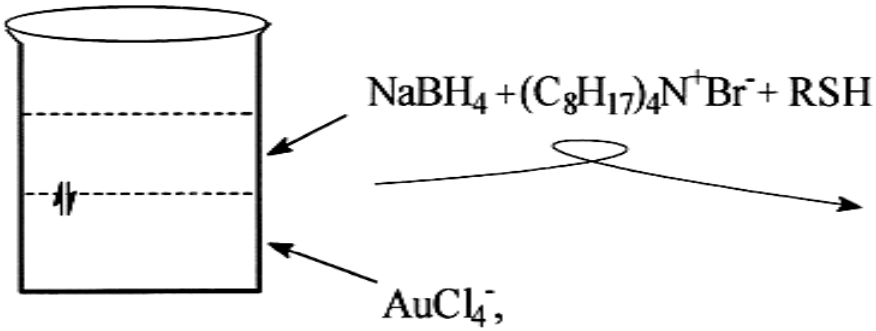

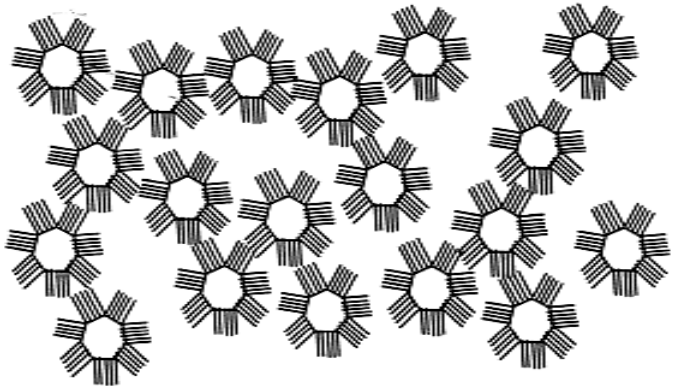

$AuCl_4^-(toluene) + RSH \longrightarrow (-Au^ISR-)_n(polymer)$

$(-Au^ISR-)_n + BH_4^- \longrightarrow Au_x(SR)_y$

M. Brust, et al *J. Chem. Soc. Chem. Commun.* **1994**, 801.

Characteristics of the Nucleation-Growth-Passivation Process:

1. Larger thiol: gold mole ratios give smaller average MPC core sizes.
2. Fast reduction and cooled solutions produce smaller, more monodispersed MPCs.
3. Quenching the reaction immediately following the reduction produces smaller core sizes.

- Core Metals: Au, Ag, Au/Ag, Au/Cu, Au/Ag/Cu, Au/Pt, Au/Pd, Au/Ag/Cu/Pd
- Ligands: Alkanethiols, disulfides, ω-functionalized thiols, arenethiols…

Reactivity of Monolayer-Protected Clusters

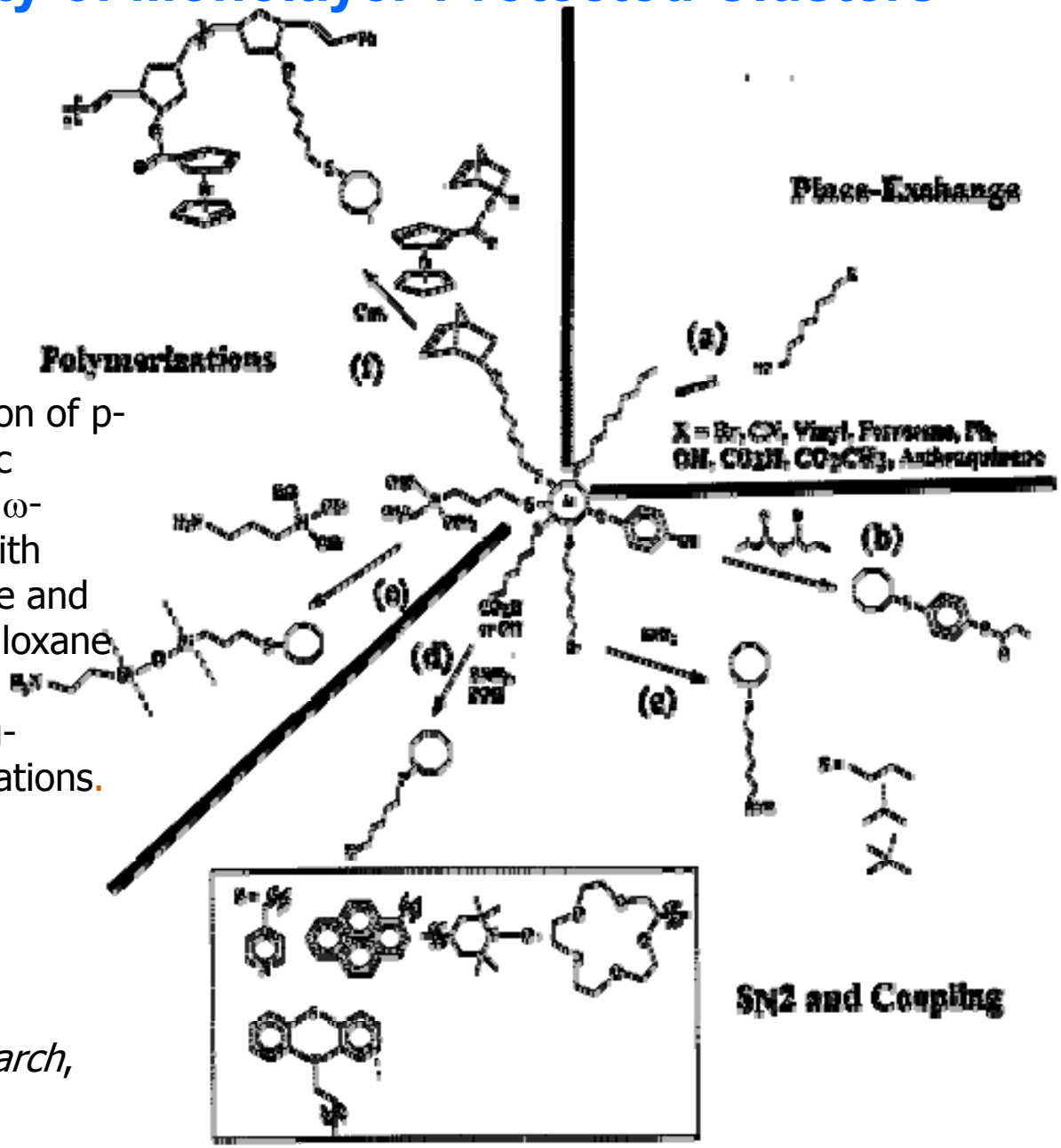

(a) Place-exchange. (b) reaction of p-mercaptophenol with propionic anhydride. (c) S_N2 reaction of ω-bromoalkanethiolated MPCs with primary alkylamines. (d) amide and ester coupling reactions. (e) siloxane formation reactions. And (f) transition-metal-catalyzed ring-opening metathesis polymerizations.

Account of Chemistry Research, V. 33 (1) P. 27

Alkanethiolate Protected Silver Clusters

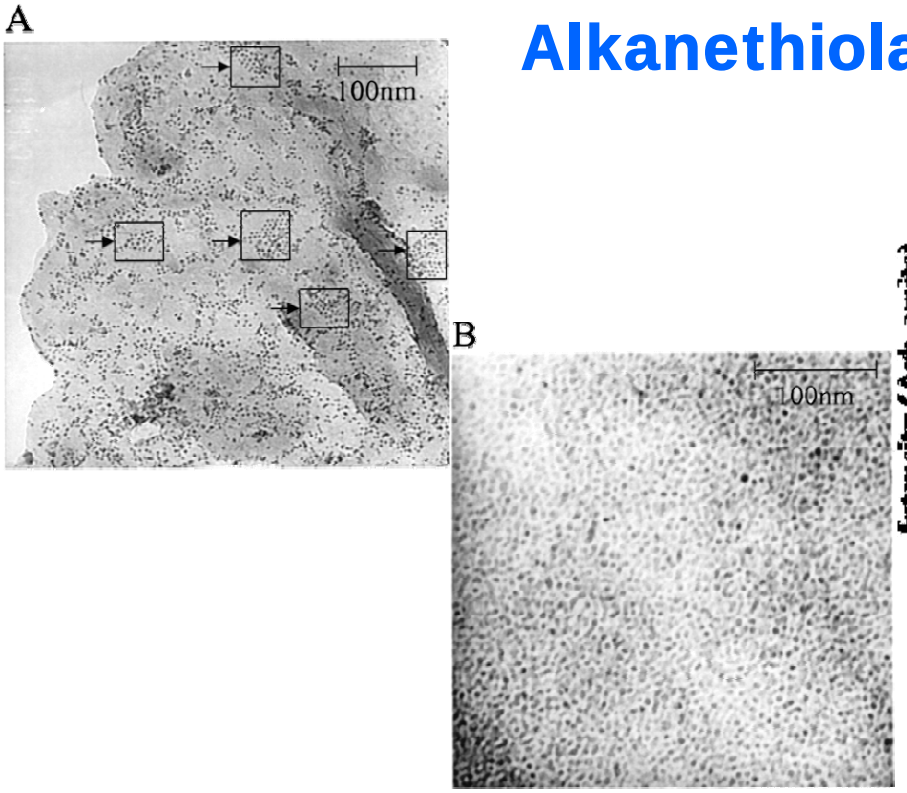

Transmission electron micrographs of octanethiol-capped Ag cluster. (A) Soluble portion of Ag-OT and slow evaporation leading to ordering. The observed (111) planes are marked. Absence of a long-range order is attributed to the polydispersity of the particles. (B) Insoluble portion after sonication in toluene. Uniform size distribution is observed.

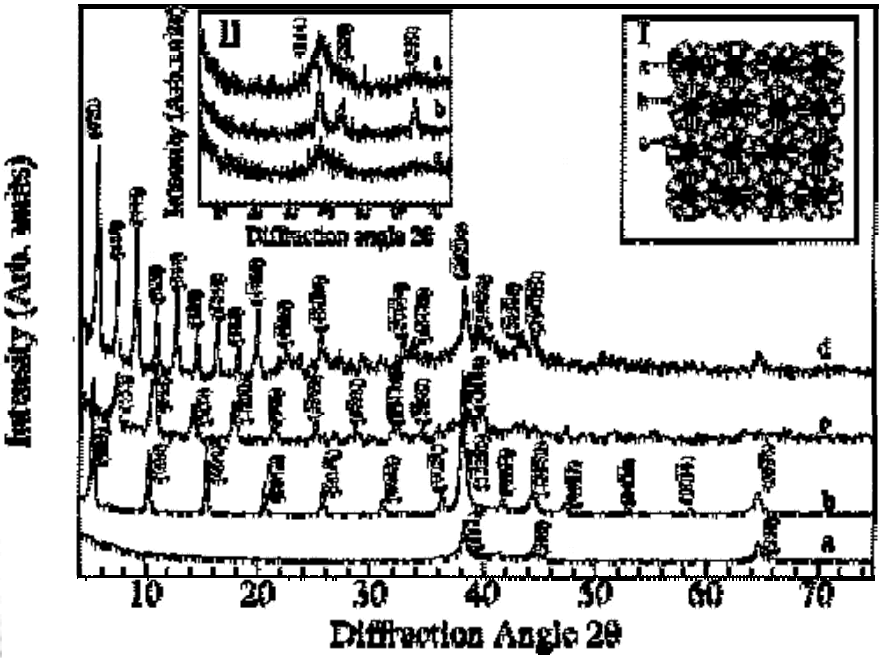

Cu K XRD patterns of (a) Ag-BT, (b) Ag-PT, (c) Ag-OT, and (d) Ag-ODT. A schematic of the super-lattice is shown in inset I. The cluster cores and the organized and unorganized alkyl chains are represented by a, b, and c, respectively. The shape of the cluster cores observed in TEM15 and the ordering of the alkyl chains seen in IR are considered in preparing this schematic. Inset II shows the XRD patterns of the Au clusters capped with (a) BT, (b) OT, and (c) ODT. The reflections are labeled.

Microcontact Printing, μCP (Whitsides et al.)

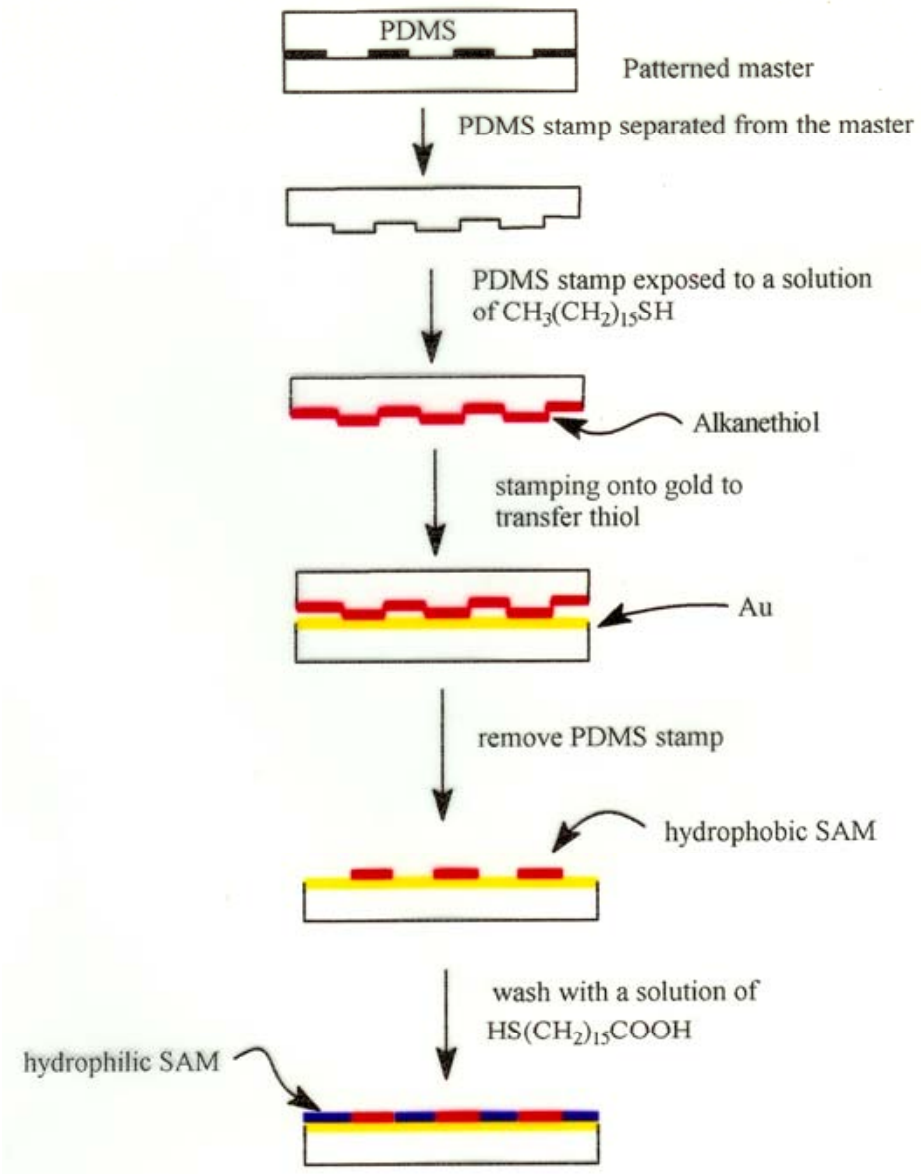

Features of PDMS as stamp:

1. The elastomer conforms to the substrate surface.
2. It has low interfacial free energy.
3. It is homogeneous, isotropic, optically transparent down to 300 nm.
4. It is durable.
5. PDMS surface can be modified by plasma treatment and SAM formation.

Problems with PDMS elastomer:

pairing, sagging, shrinking, swelling…

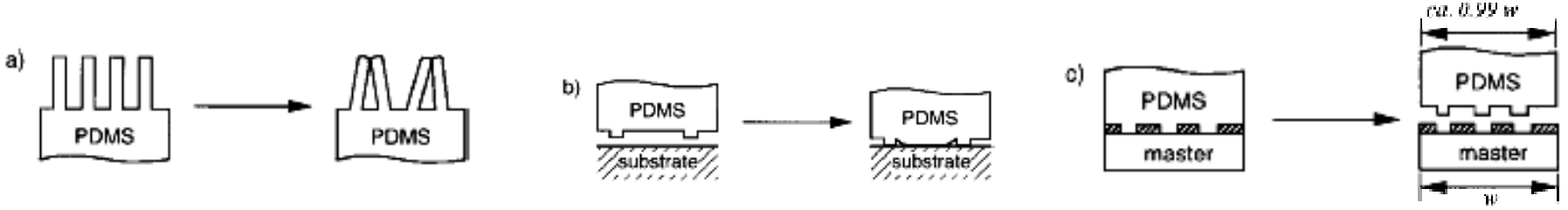

Features of thiolate in ethanol as the ink:

- ♦ Fast reaction,
- ♦ Autophobicity of the SAM surface

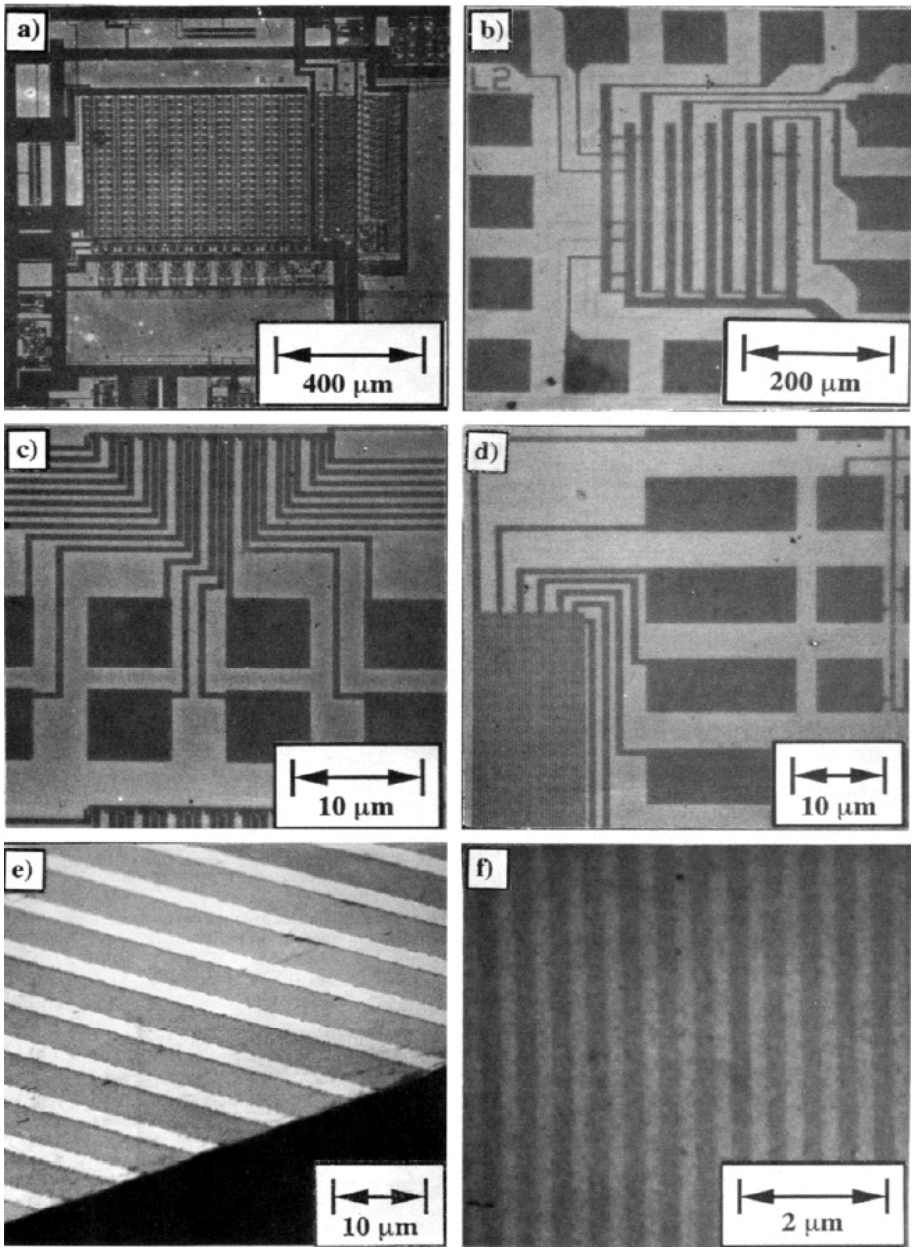

SEM micrographs of several types of structures formed through rubber stamping and chemical etching (a-d). (e) Fracture profile of a series of gold lines supported on a silicon wafer. The width of the gold lines is 2μm, and the thickness of the gold is 2000Å. The tilt allows observation of the thickness of the gold and the resolution of the edge. (f) The smallest features that are currently accessible using rubber stamping. The width of the lines is 0.2μm. Although the arrays with features on scales of 1μm or greater are easy to produce, the arrays of submicrometer (0.2 μm) lines are not routinely reproducible through rubber stamping by hand: they represent best-case examples, and the view shown was chosen from regions of lower fidelity. More precise mechanical control should allow these arrays to be produced with better reproducibility.

Langmuir, 1994, V. 10 (5) P. 1503

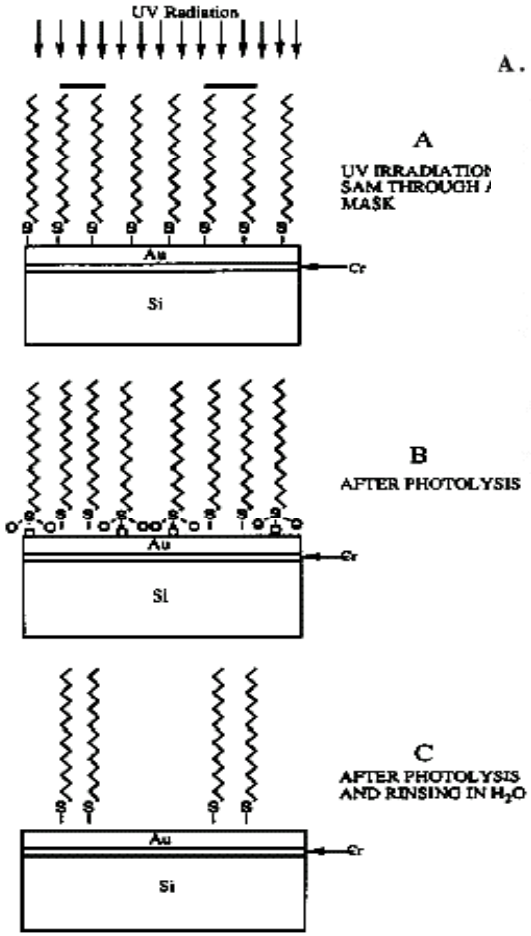

Diagrams illustrating the concepts underlying the use of alkanethiol SAMs as monolayer photoresists on gold. (A) The self-assembled monolayer is formed providing a protective coating for the gold. (B) The SAM is photolyzed in air generating alkylsulfonates in the regions exposed to UV radiation. (C) The alkylsulfonates can be rinsed off of the surface with distilled water exposing the gold for subsequent processing.

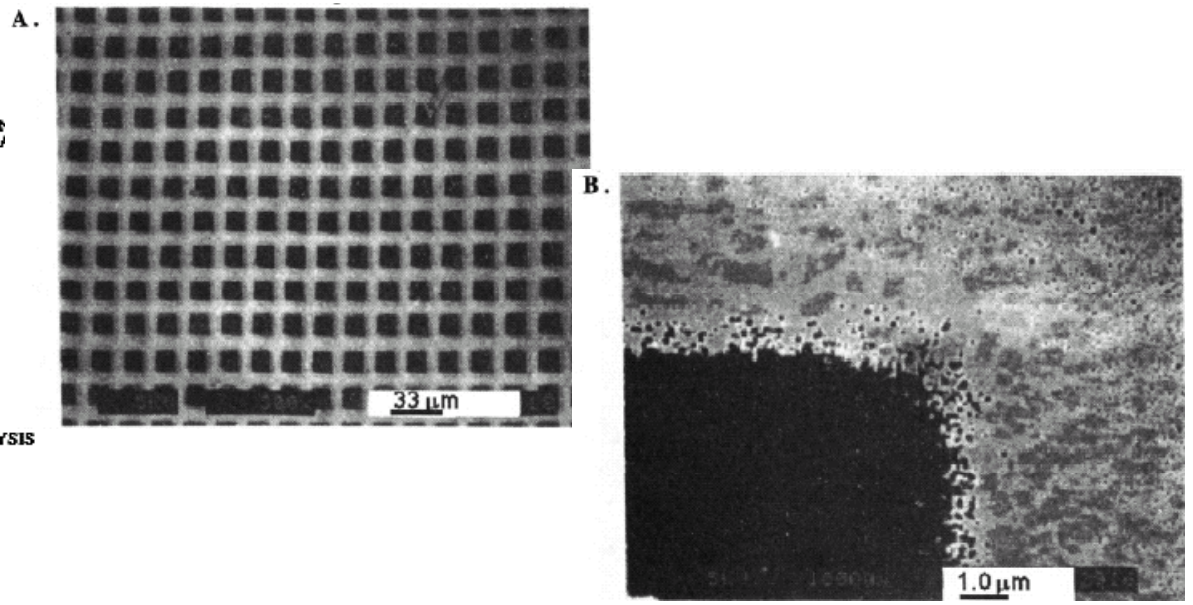

Scanning electron microscopy images of the sample patterned as described in the text. Light areas were protected from UV exposure by the grid type mask. Dark areas are where the gold has been removed by the acid etching step. (A) A 33μm marker is shown in the lower right of the image. The gold lines are ~5-6 μm across, replicating the mask dimensions. (B) This higher resolution image shows the edge of a gold line providing an indication of the scale of the damage at the edge of a line. A 1.0 μm marker is shown in the lower right of the image.

J. Huang, D.A. Dahlgren, J. C. Hemminger, *Langmuir*, 1994, V. 10 (3), 626-628

Dip Pen Nanolithography

A coated tip is translated along a surface depositing molecules in its wake...

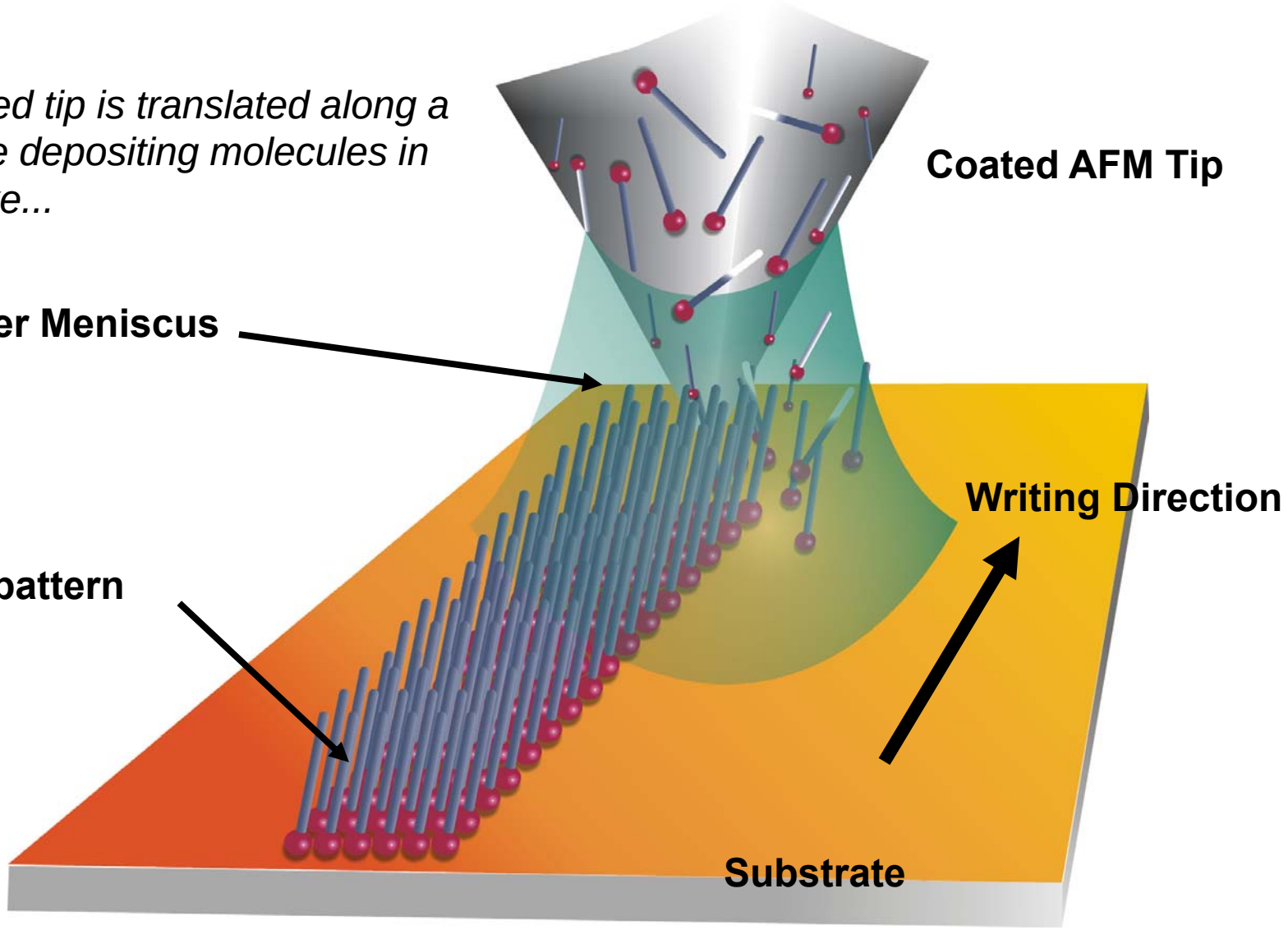

Pattern Size Control with DPN

❖ **Area of the Final Patterns 🔔 Contact Time between Tip and Sample**

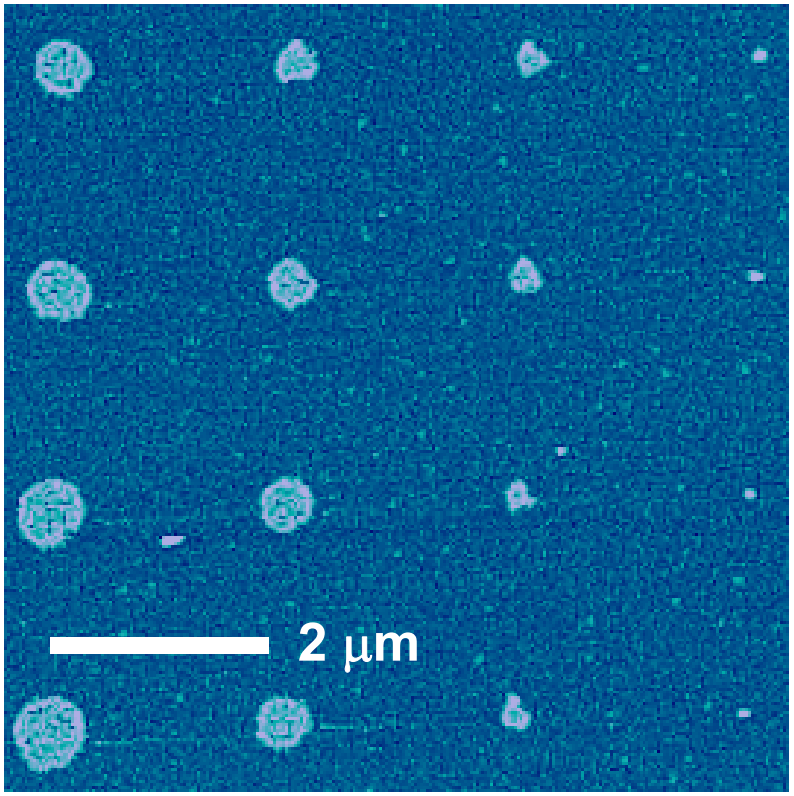

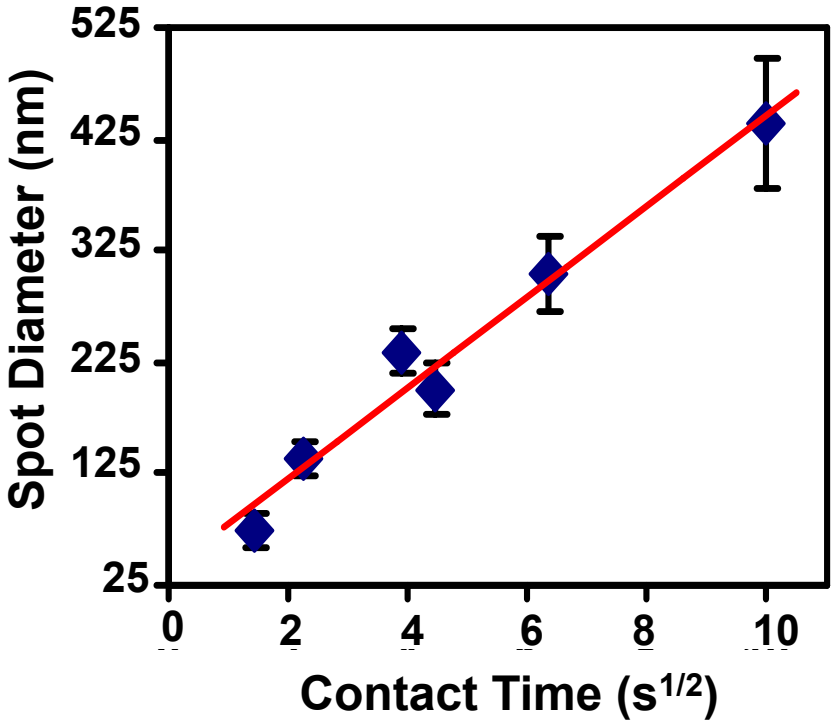

DNA patterned on gold w/ nanoparticle labels

Demers, L. M. et al. *Science* 298, 1836-1838 (2002).

Affect of Temperature and Humidity

- Control over relative humidity and temperature enables precise calibration of feature size

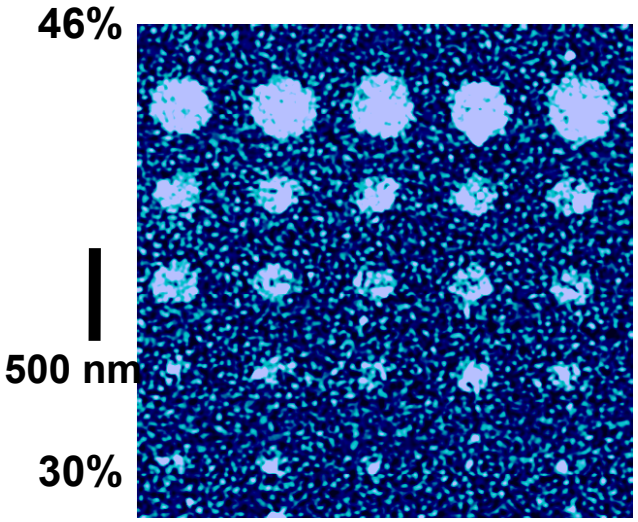

DNA patterned on Au at varied relative humidity

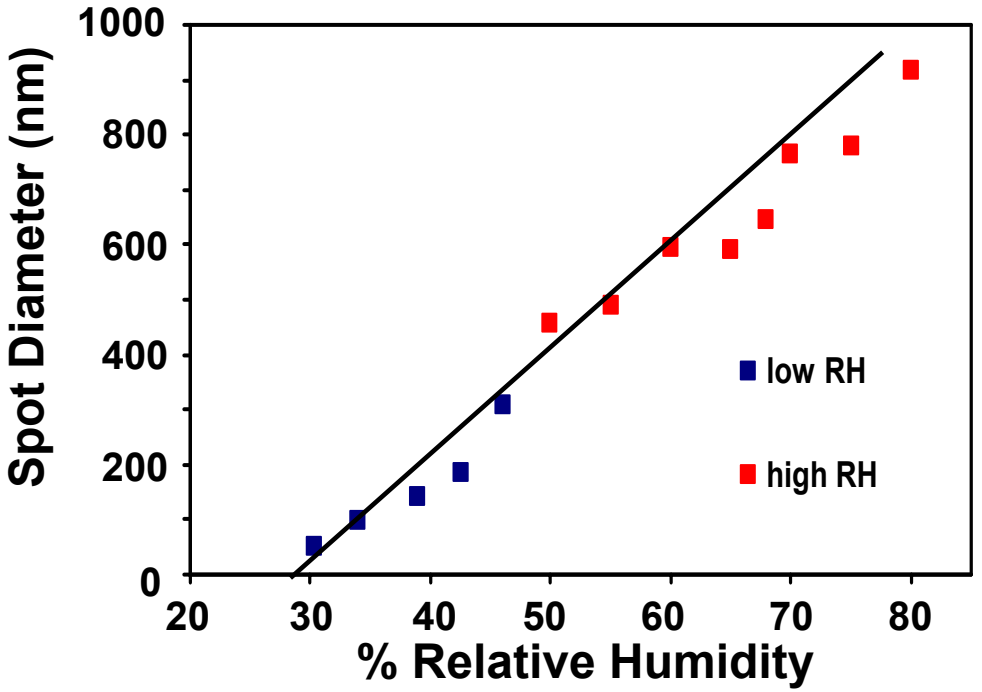

Demers, L. M. et al. *Science* 298, 1836-1838 (2002).

Combinatorial Study Using Multiple Nanostructures Made of Different Inks

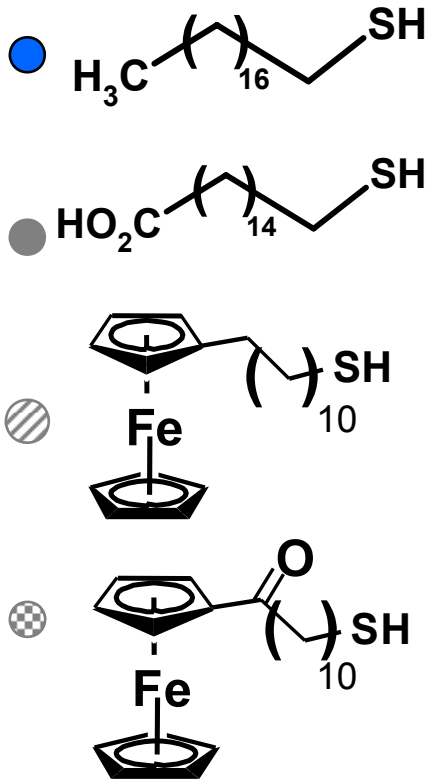

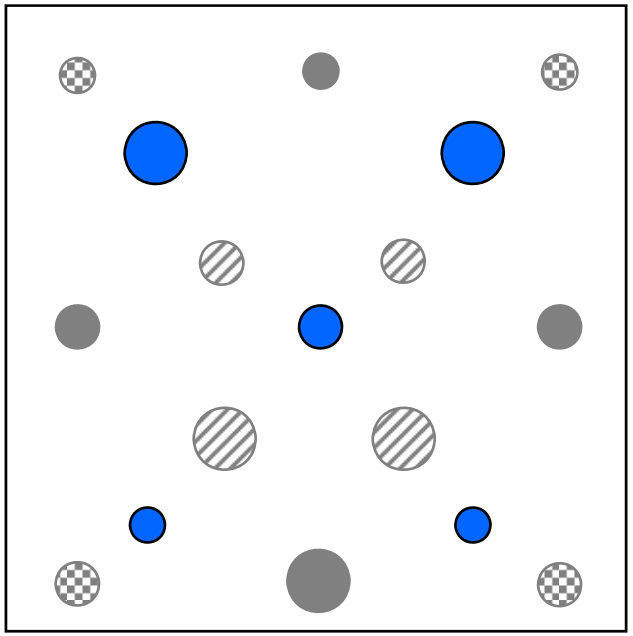

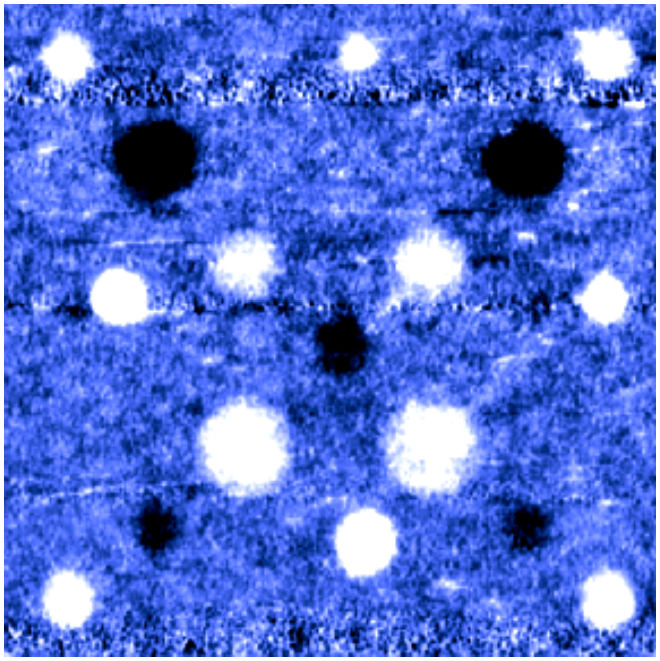

Ivanisevic, A. et al *J. Am. Chem. Soc.* 124, 11997-12001 (2002).

DPN Inks

- Soft Materials
  - Small functional molecules
  - SAMs (e.g. alkanethiols, silanes), etch barriers
  - Conducting polymers
  - Biopolymers (eg. DNA, proteins, peptides)
- Hard Materials
  - Metal inks
  - Sol precursor inorganic inks (SiOx, SnOx, BaFe, etc)
  - Nanoparticle catalysts

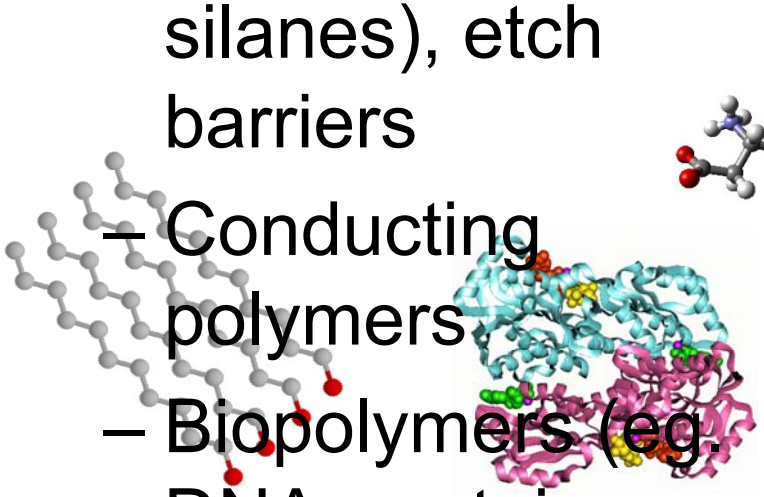

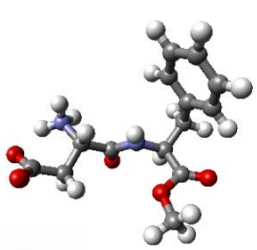

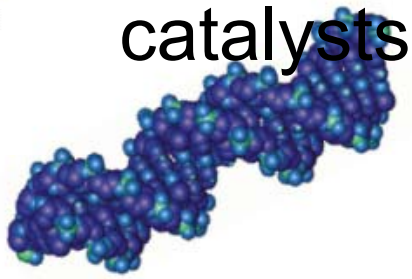

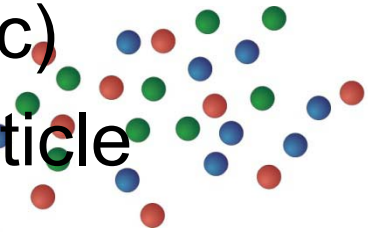

Etch Barriers for Solid-State Nanostructures

1. "Write" regions of octadecanethiol (ODT) on Au thin film.

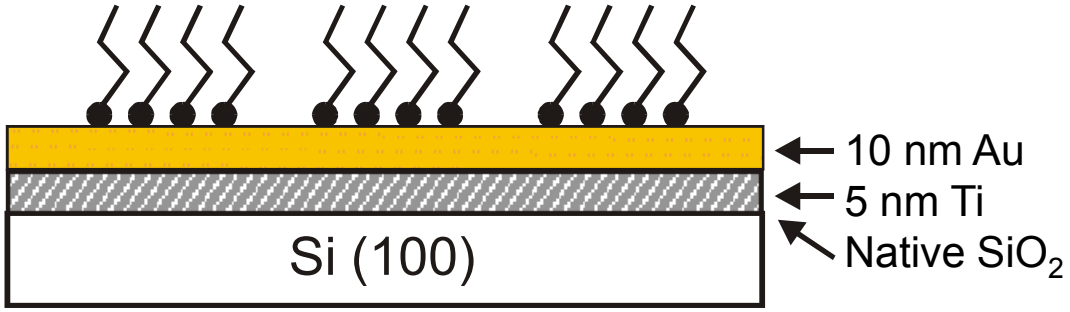

2. Selectively etch Au using wet chemical etchant (ferri/ferrocyanide 2-5 min).

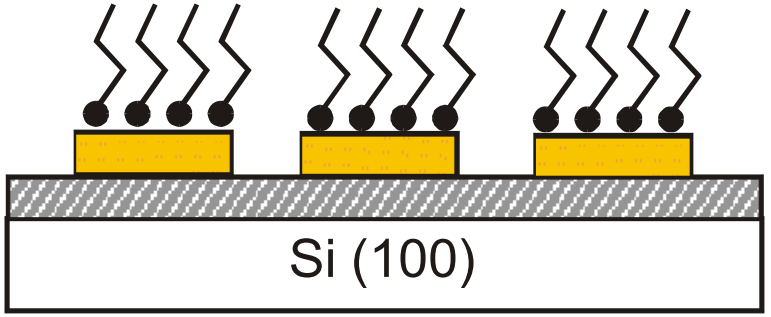

3. Remove Ti and SiO_2, etch Si, and passivate Si surface.

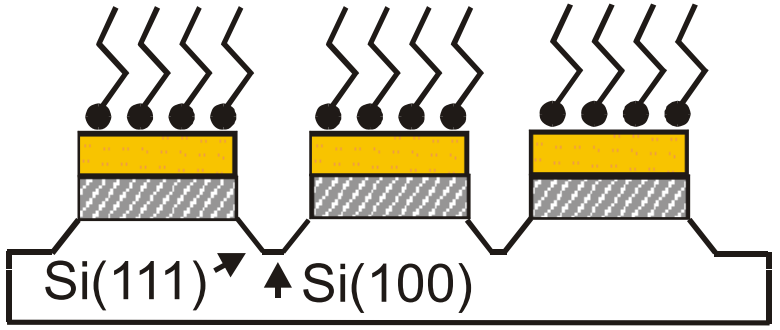

Weinberger, D. A., et al *Adv. Mater.* 12, 1600-1603 (2000).

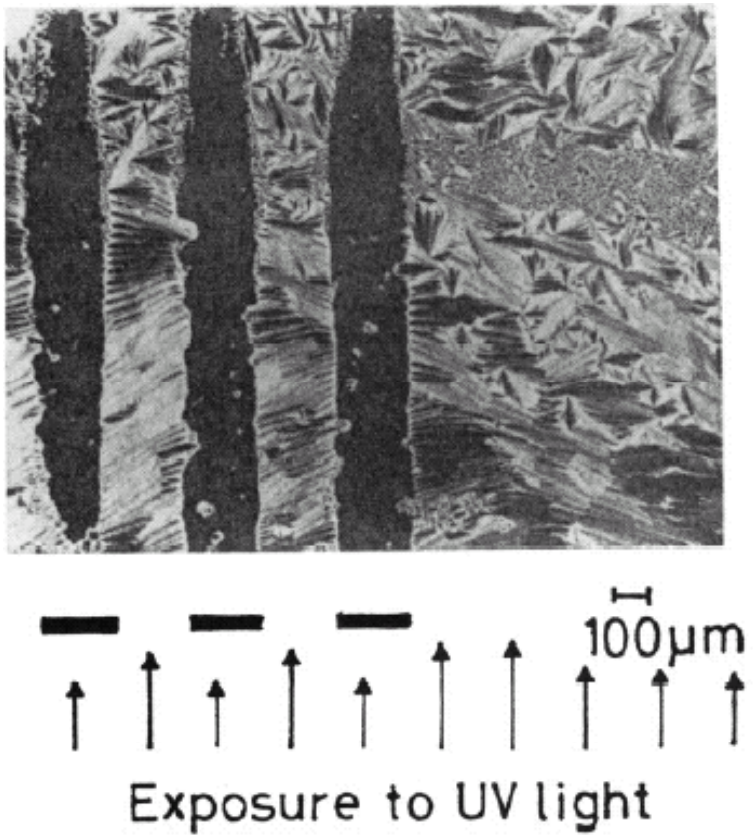

Polarized photomicrograph of a cell of 8μm thickness exposed to UV through a 200-μm lines and spaces photomask.

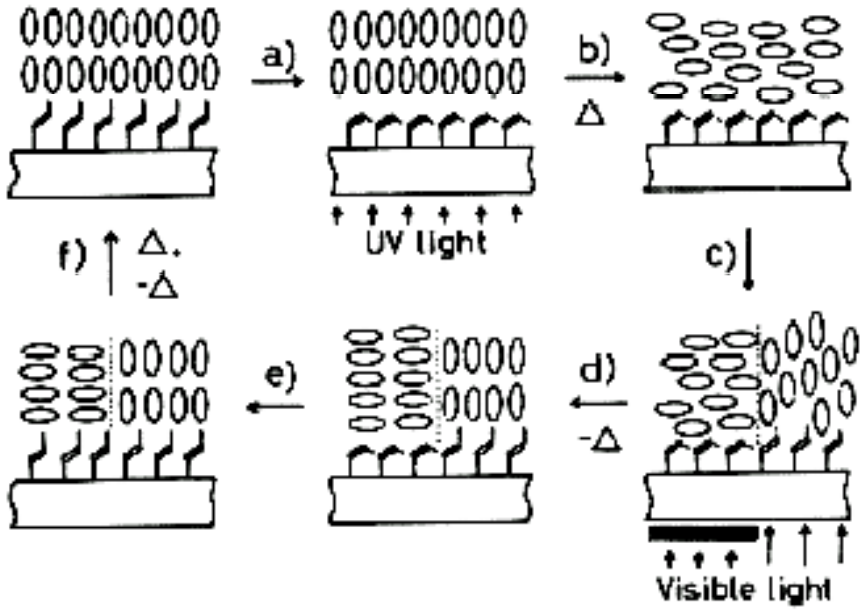

Schematic representation of an erasable optical information storage using a photoresponsive smectic LC cell: (a) initialization by UV exposure in the smectic phase; (b) heat above T_{SN} to cause planar alignment in the nematic phase; (c) subsequent writing-in with visible light in the nematic phase; (d) rapid cooling down for fixation; (e) memory storage below T_{SN}; (f) erasure by heating.

Electronic properties of SAMs

♦Electron Transfer through molecules, studied by STM tip or conductive AFM tip on a well-defined, oriented SAM.

♦use of SAM for modifying electronic interface properties in a heterostructure.

Are Single Molecular Wires Conducting?

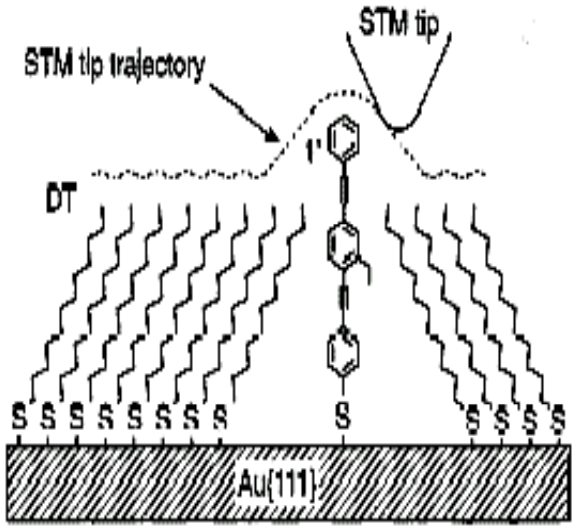

A schematic representation of a DT and 1' SAM on Au{111}. The height that the 1' molecule extends above the DT film, if normal to the surface, is 7.3Å. The trajectory of the STM tip traces out a surface of constant current. The relatively flat DT layer can be imaged by an atomic scale asperity on the end of the STM tip with resolution of the molecular lattice. The protruding 1' molecule "images" the end of the STM tip, resulting in a characteristic feature due largely to the shape of the end of the STM tip for each 1' molecule. The STM tip is closer to the exposed ends of the 1' molecules then to the exposed ends of the DT molecules because the ATBH is higher over the 1' molecules than over the DT molecules.

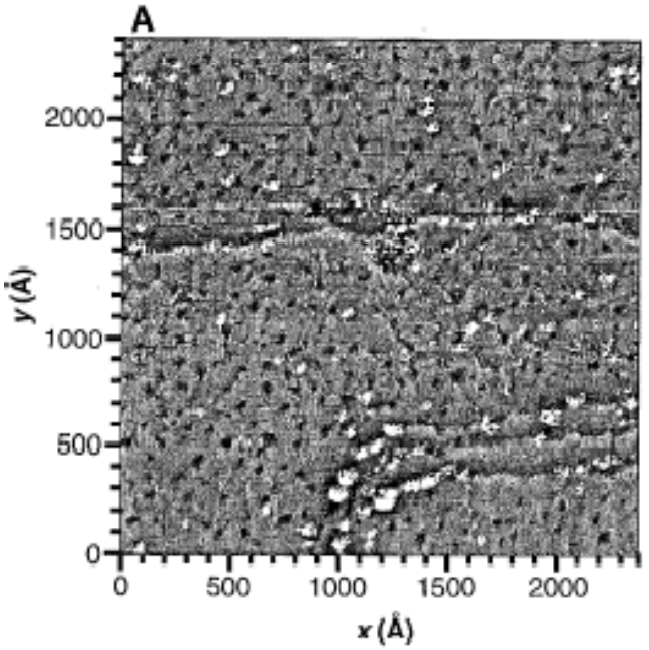

Constant-current STM topographs of an Au{111} surface covered by DT and 1' molecules (tip bias, 1.0V; tunneling current, 10pÅ.)

Science, 1996, V. 271 (5256) P. 1705-1707

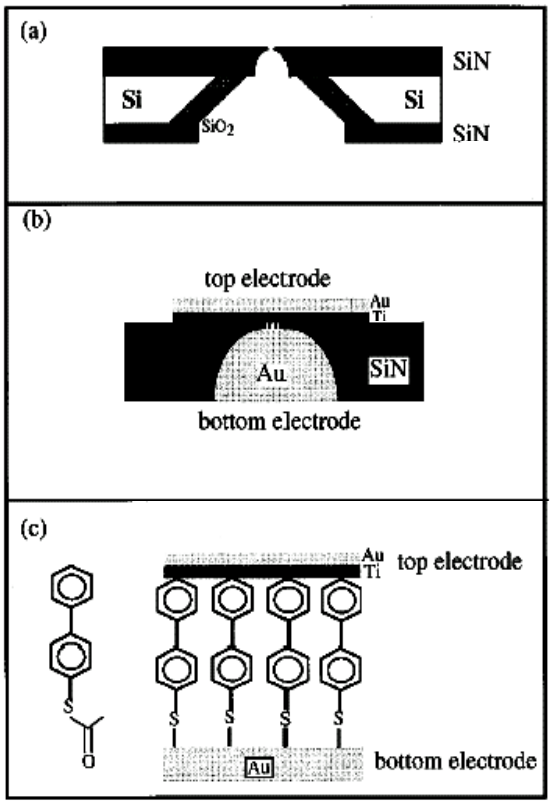

Fabrication of the heterostructure. (a) cross section of a silicon wafer showing the bowl-shaped pore etched in suspended SiN membrane with a diameter about 300Å. (b) Au-Ti top electrode/self-assembled monolayer/ Au bottom electrode sandwich structure in the nanopore. (c) 4-thioacetylbiphenyl and detail diagram of the sandwich heterostructure.

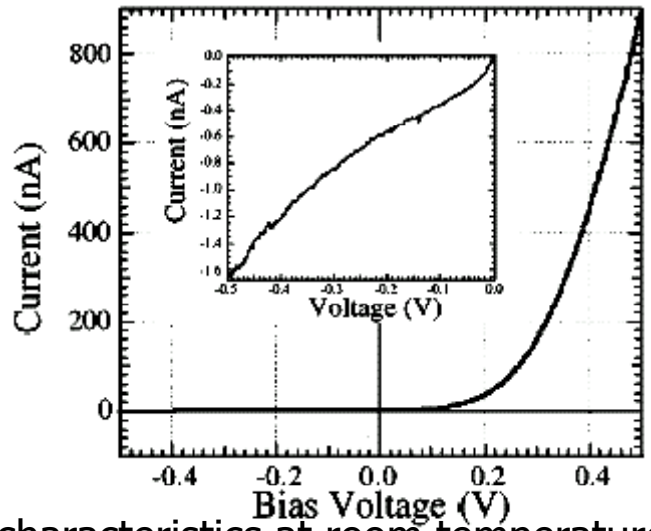

I-V characteristics at room temperature. Magnified view of the negative bias part in the inset.

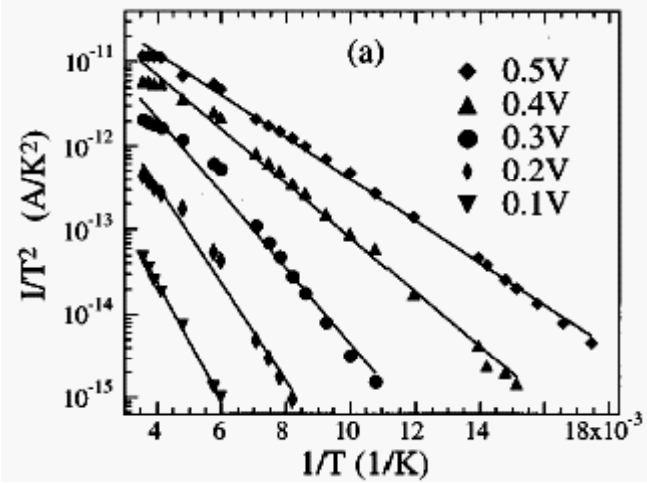

Plots of $1/T^2$ vs $1/T$ for a series of positive bias voltages. The straight lines are least-square fits to the data points for each bias.

Applied Physics Letters, 1997, V 71 (5) P. 611